J Physiol 596.11 (2018) pp 2091–2120

The Journal of Physiology

Effect of resistance training and protein intake pattern on myofibrillar protein synthesis and proteome kinetics in older men in energy restriction

Caoileann H. Murphy[1,*], Mahalakshmi Shankaran[2,7,*], Tyler A. Churchward-Venne[1], Cameron J. Mitchell[1], Nathan M. Kolar[1], Louise M. Burke[3], John A. Hawley[4,5], Amira Kassis[6], Leonidas G. Karagounis[6], Kelvin Li[2,7], Chelsea King[2], Marc Hellerstein[2,7] and Stuart M. Phillips[1]

[1] *Department of Kinesiology, McMaster University, Canada*
[2] *KineMed, Inc., Emeryville, CA, USA*
[3] *Department of Sports Nutrition, Australian Institute of Sport, Canberra, Australia*
[4] *Exercise and Nutrition Research Group, Mary MacKillop Institute for Health Research, Australian Catholic University, Victoria, Australia*
[5] *Research Institute for Sport and Exercise Sciences, Liverpool John Moores University, UK*
[6] *Nestlé Research Center, Nestec Ltd, Lausanne, Switzerland*
[7] *Department of Nutritional Sciences and Toxicology, University of California, Berkeley, CA, USA*

Edited by: Scott Powers & Troy Hornberger

Key points

- Strategies to enhance the loss of fat while preserving muscle mass during energy restriction are of great importance to prevent sarcopenia in overweight older adults.
- We show for the first time that the integrated rate of synthesis of numerous individual contractile, cytosolic and mitochondrial skeletal muscle proteins was increased by resistance training (RT) and unaffected by dietary protein intake pattern during energy restriction in free-living, obese older men.
- We observed a correlation between the synthetic rates of skeletal muscle-derived proteins obtained in serum (creatine kinase M-type, carbonic anhydrase 3) and the synthetic rates of proteins obtained via muscle sampling; and that the synthesis rates of these proteins in serum revealed the stimulatory effects of RT.
- These results have ramifications for understanding the influence of RT on skeletal muscle and are consistent with the role of RT in maintaining muscle protein synthesis and potentially supporting muscle mass preservation during weight loss.

Abstract We determined how the pattern of protein intake and resistance training (RT) influenced longer-term (2 weeks) integrated myofibrillar protein synthesis (MyoPS) during energy restriction (ER). MyoPS and proteome kinetics were measured during 2 weeks of ER alone and 2 weeks of ER plus RT (ER + RT) in overweight/obese older men. Participants were randomized

Caoileann Murphy trained as a Dietitian in Trinity College Dublin. After qualifying in 2009 she worked clinically at St. James's Hospital in Dublin before deciding to complete a Masters in Sport and Exercise Nutrition at Loughborough University in the UK. Following this Caoileann completing her PhD in nutrition and exercise strategies to maximize rates of muscle protein synthesis and counter sarcopenia in McMaster University, Canada, under the supervision of Professor Stuart Phillips. Caoileann now works as a Postdoctoral Research Fellow in the Nutrigenomics Research Group led by Professor Helen Roche in University College Dublin. Her postdoctoral research is in the area of nutrition and sarcopenia with an emphasis on personalized approaches to effective treatment and prevention. Caoileann is a recipient of the TOPMed10 Marie Curie Fellowship and the ESPEN Fellowship 2017.

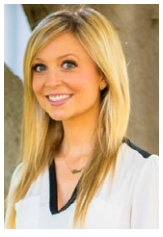

*These two authors contributed equally to the work.

DOI: 10.1113/JP275246

to consume dietary protein in a balanced (BAL: 25% daily protein per meal × 4 meals) or skewed (SKEW: 7:17:72:4% daily protein per meal) pattern ($n = 10$ per group). Participants ingested deuterated water during the consecutive 2-week periods, and skeletal muscle biopsies and serum were obtained at the beginning and conclusion of ER and ER + RT. Bulk MyoPS (i.e. synthesis of the myofibrillar protein sub-fraction) and the synthetic rates of numerous individual skeletal muscle proteins were quantified. Bulk MyoPS was not affected by protein distribution during ER or ER + RT (ER: BAL = 1.24 ± 0.31%/day, SKEW = 1.26 ± 0.37%/day; ER + RT: BAL = 1.64 ± 0.48%/day, SKEW = 1.52 ± 0.66%/day) but was ∼26% higher during ER + RT than during ER ($P = 0.023$). The synthetic rates of 175 of 190 contractile, cytosolic and mitochondrial skeletal muscle proteins, as well as synthesis of muscle-derived proteins measured in serum, creatine kinase M-type (CK-M) and carbonic anhydrase 3 (CA-3), were higher during ER + RT than during ER ($P < 0.05$). In addition, the synthetic rates of CK-M and CA-3 measured in serum correlated with the synthetic rates of proteins obtained via muscle sampling ($P < 0.05$). This study provides novel data on the skeletal muscle adaptations to RT and dietary protein distribution.

(Resubmitted 8 September 2017; accepted after revision 20 February 2018; first published online 12 March 2018)
Corresponding author S. M. Phillips: Department of Kinesiology, Exercise Metabolism Research Group, McMaster University, 1280 Main St. West, Hamilton, ON, Canada. Email: phillis@mcmaster.ca

Introduction

Sarcopenia, the progressive loss of skeletal muscle mass with age, is associated with a decline in strength and functional capacity, and increased risk for numerous adverse health and quality of life-based outcomes (Janssen *et al.* 2004; Landi *et al.* 2013). Sarcopenia is often concomitant with obesity in older adults (Diouf *et al.* 2010; Flegal *et al.* 2012; Gutierrez-Fisac *et al.* 2012; Parr *et al.* 2013). In older adults obesity is associated with increased risk for comorbidities (Nicklas *et al.* 2006; Rossi *et al.* 2008; Mathus-Vliegen, 2012) and exacerbates age-related functional decline and disability risk (Vasquez *et al.* 2014), particularly when superimposed on sarcopenia (Baumgartner *et al.* 2004; Chung *et al.* 2013). The recommendation of weight loss in overweight older adults remains somewhat controversial (Waters *et al.* 2013), primarily due to concerns that dietary energy restriction (ER) interventions designed to reduce excess adiposity may simultaneously accelerate muscle loss (Bouchonville & Villareal, 2013; Waters *et al.* 2013).

Both ageing (Moore *et al.* 2015) and ER (Hector *et al.* 2015) have been shown to attenuate the acute muscle protein synthetic response to protein feeding. We reported that during ER in overweight and obese older men a balanced distribution of dietary protein ingestion more effectively stimulated myofibrillar protein synthesis (MyoPS) *versus* a skewed distribution (Murphy *et al.* 2015). Furthermore, we showed that combining resistance training (RT) with a balanced protein distribution restored the reduced rates of MyoPS during ER to those observed during energy balance (EB). These data suggest that the combination of RT and a balanced distribution of daily protein during ER may represent an effective strategy to slow or abate muscle loss during weight loss in older adults. Nevertheless, the short-term (11 h) nature of the MyoPS measurements in that study (Murphy *et al.* 2015) restricted our ability to extrapolate these findings because they do not account for all of the integrated aspects of daily activity and diet over time. To overcome this limitation, we simultaneously administered oral deuterated water (D_2O) to the participants in our previous study (Murphy *et al.* 2015). This represents a more powerful approach to determine muscle protein synthesis (MPS) over longer periods of time (weeks or longer) and, using recently developed methods combining D_2O ingestion with tandem-mass spectrometric proteomic analyses, permits the measurement of the synthetic rates of a large number of individual skeletal muscle proteins (Price *et al.* 2012; Scalzo *et al.* 2014). Such methodology can capture the time-integrated responses of skeletal muscle protein synthesis across the proteome, including numerous myofibrillar, sarcoplasmic and mitochondrial proteins, to an intervention among free-living participants, thereby providing unique insight into skeletal muscle adaptations. We have recently extended this approach to measure the synthetic rate of skeletal muscle-synthesized proteins that escape into circulation such as creatine kinase M-type (CK-M) and carbonic anhydrase (CA-3) (Shankaran *et al.* 2016*a*). The underlying concept is that the synthetic rates of blood-borne proteins that were synthesized in skeletal muscle can provide a minimally invasive biomarker of MPS (Shankaran *et al.* 2016*a*) and, if successful, could have implications for the diagnosis, clinical management and monitoring of musculoskeletal diseases.

The purpose of the current study was to examine the interaction between daily protein distribution and RT on the longer-term, integrated rate of bulk MyoPS (i.e. synthesis of the myofibrillar protein sub-fraction) and on the synthetic rates of individual skeletal muscle proteins in

the setting of ER. The study design comprised 2 weeks of ER alone and 2 weeks of ER + RT, combined with either a skewed or balanced dietary protein intake pattern, in the overweight and obese older men who took part in our previous study (Murphy *et al.* 2015). Based on our previous findings (Murphy *et al.* 2015), we hypothesized that a balanced distribution of dietary protein intake throughout the day would stimulate the longer-term synthesis rate of bulk MyoPS and the synthesis rates of individual myofibrillar skeletal muscle proteins (%/day) to a greater extent than a skewed distribution and that this effect would be enhanced while undertaking RT.

Methods

Ethical approval

This study was approved by the Hamilton Integrated Research Ethics Board and conformed to the standards set by the Declaration of Helsinki, except for registration in a database. Each participant was informed of the purpose of the study, experimental procedures and potential risks before written consent was obtained.

Experimental design

Details regarding the participants and controlled diet and physical activity interventions have been reported previously (Murphy *et al.* 2015). Briefly, after providing informed, written consent, 20 overweight and obese but generally healthy older men [age 66 ± 4 years, body mass index (BMI) 31 ± 5 kg/m^2) underwent a controlled 4-week hypocaloric diet (1.25 MJ/d less than estimated energy requirements, 1.3 g protein/kg/d from a mixture of plant and animal sources; Fig. 1). Participants were randomly allocated to one of two groups (n = 10 per group) matched for age and BMI: balanced (BAL) or skewed (SKEW). Total protein intake was distributed across four daily meals (breakfast, lunch, dinner, pre-bed snack) in the proportions 25:25:25:25% in participants in the BAL group and 7:17:72:4% in the SKEW group. In BAL, a ready-to-drink whey protein micelle (WPM) beverage (25 g protein; Nestle, Lausanne, Switzerland) was consumed as part of breakfast and as a pre-bed snack to achieve target protein intakes at these meals. SKEW received their total daily protein intake from food sources only and consumed a protein-free, low-energy placebo drink (0.2 g protein; Nestle) matched for appearance, smell and taste to the WPM beverage with breakfast and pre-bed. The 4-week intervention consisted of two, 2-week phases. In weeks 1 and 2 all participants were in energy restriction (Phase 1: ER) and continued their habitual physical activity. In weeks 3 and 4, while still energy restricted, all participants commenced a supervised, whole body, resistance training programme 3 days per week (Phase 2: ER + RT).

Stable isotope labelling protocol

Deuterated water (D_2O, ^2H_2O) labelling of newly synthesized skeletal muscle proteins was achieved using daily oral consumption of aliquots of 70% D_2O. This commenced on the first day of the ER diet and was continued throughout the 4-week intervention. A target deuterium (^2H) enrichment in total body water of 1–2% was achieved during the first 5 days by intake of 60 mL 70% D_2O three times/day (= 180 mL/day) and was

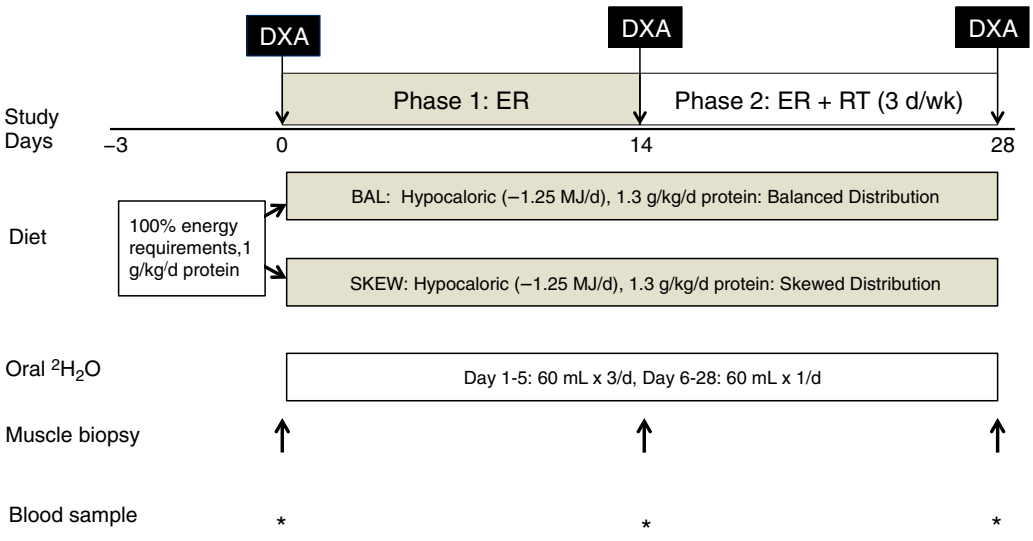

Figure 1. Schematic overview of the study design (adapted from Murphy *et al.* 2015)
DXA, dual X-ray absorptiometry; EB, energy balance; ER, energy restriction; ER + RT, energy restriction and resistance training. [Colour figure can be viewed at wileyonlinelibrary.com]

maintained for the remaining 23 days of the intervention by 60 mL/day. All 60 mL doses were separated by at least 3 h. All participants tolerated the D_2O dosing protocol well and no one reported side effects (i.e. nausea, vertigo). Total body water ^2H enrichment can be used as a surrogate for tissue amino acid labelling (Robinson *et al.* 2011; Scalzo *et al.* 2014; Wilkinson *et al.* 2014) and was determined from saliva swabs collected on alternate days throughout the 4-week labelling period, as described previously (Neese *et al.* 2001; Turner *et al.* 2003). Participants were instructed not to eat or drink for 30 min before saliva sampling and samples were stored at −80°C until analysis. Blood samples and muscle biopsies from the vastus lateralis were obtained on days 0 (baseline), 14 (end of Phase 1: ER; baseline of Phase 2: ER + RT) and 28 (end of Phase 2: ER + RT) (Fig. 1).

Body water enrichment

Enrichment of ^2H in saliva was determined using a previously described method (Price *et al.* 2012). Saliva samples were diluted 1:100 and placed into the caps of inverted sealed screw-capped vials for overnight distillation at 80°C. Body water ^2H enrichments were determined by direct measurement of deuterium molar percentage excess (MPE) in water distilled from the saliva against a D_2O standard curve using a laser water isotope analyser (Los Gatos Research, Los Gatos, CA, USA).

Bulk myofibrillar protein synthesis

Myofibrillar-enriched proteins were isolated as previously described (Moore *et al.* 2009). Amino acids were liberated by adding 1 M HCl and DOWEX (50WX8-200 resin, Sigma-Aldrich, Poole, UK) and heating at 110°C for 72 h, with vortex mixing every 24 h. Free amino acids were purified using DOWEX ion exchange chromatography and converted to their pentafluorobenzyl-N,N-di(pentafluorobenzyl)-NEAA derivatives (PFB derivatives) as described previously (Busch *et al.* 2006). Gas chromatography mass spectrometry (GCMS) was performed in negative chemical ionization mode with helium as the carrier gas, and mass-to-charge (m/z) ratios 424–426 corresponding to the M0, M1 and M2 mass isotopomers of derivatized alanine were analysed by selected ion monitoring.

Excess fractional M + 1 enrichment (EM1) was the normalized change in isotopomer intensity calculated as:

$$\mathrm{EM1} = [(\mathrm{M1})_{\mathrm{sample}}/(\mathrm{M0}+\mathrm{M1})_{\mathrm{sample}}] - [(\mathrm{M1})_{\mathrm{standard}}/(\mathrm{M0}+\mathrm{M1})_{\mathrm{standard}}]$$

where sample and standard refer to the sample and an unenriched pentafluorobenzyl triacetyl alanine derivative, respectively. The fraction of bulk myofibrillar protein that was newly synthesized during the labelling period (f) was calculated as the ratio of the measured EM1 to the asymptotic value of EM1 ($\mathrm{EM1}_{\mathrm{max}}$), the latter representing EM1 in alanine in fully turned-over proteins at the time-averaged ^2H_2O enrichment for each sample and calculated as $f = \mathrm{EM1}_{\mathrm{sample}}/\mathrm{EM1}_{\mathrm{max}}$, as described previously (Busch *et al.* 2006).

To calculate absolute rates of whole body bulk MyoPS, skeletal muscle mass was estimated according to the model of Kim *et al.* (2002) using dual energy X-ray absorptiometry (QDR-4500A, software version 12.31, Hologic, Bedford, MA, USA) scans obtained at baseline, at the end of Phase 1: ER and at the end of Phase 2: ER + RT. Assuming that muscles are 18% protein and myofibrillar protein accounts for 66% of the total, we calculated whole body bulk MyoPS in g/day as shown by the following equation (Cuthbertson *et al.* 2005): absolute rate of bulk MyoPS (g/day) = [(muscle mass (kg) × proportion of myofibrillar protein per kg muscle) × myofibrillar fractional synthetic rate (FSR) (%/day)] × 1000.

SDS-PAGE fractionation, Coomassie blue staining and in-gel trypsin digestion of muscle proteins for analysis of skeletal muscle proteome dynamics

Muscle samples were processed as described previously (Shankaran *et al.* 2016*a*). Briefly, samples were thawed and homogenized for 75 s in PBS containing 1 mM phenylmethylsulfonyl fluoride (PMSF) and 5 mM EDTA using a Mini-BeadBeater 8 (BioSpec, Bartlesville, OK, USA) placed on ice for 1 min. This procedure was repeated twice and the resulting homogenate was diluted to 10% (w/v) in PBS containing 1 mM PMSF. Protein from prepared homogenates was uniformly reduced by incubation in 10 mM DTT and SDS-PAGE sample loading buffer for 5 min at 95°C. The reduced samples were then alkylated by incubating in 15 mM iodoacetamide for 1 h at room temperature. Proteins were then fractionated by SDS-PAGE (BioRad, Hercules, CA, USA). The gel bands corresponding to 10 discrete molecular weight regions were excised from Coomassie blue–stained gels and digested overnight with trypsin (Proteomics Grade, Sigma-Aldrich) at 37°C. The peptides were extracted from the gel, dried and reconstituted in 3% acetonitrile/0.1% formic acid for LC/MS analysis.

Immunoprecipitation of CK-M and CA-3 from serum, and in-solution trypsin digestion

Plasma samples were processed as described previously (Shankaran *et al.* 2016*a*). Briefly, CK-M and CA-3 were immunoprecipitated from 2 mL human serum using 20 μg of goat anti-CK-M polyclonal antibody (CalBioreagents, P195; Foster City, CA, USA) and 20 μg of goat anti-CA-3 polyclonal antibody (R&D Systems, AF2185; Minneapolis,

MN, USA) conjugated to 1 mg epoxy Dynabeads (Invitrogen, Carlsbad, CA, USA). Samples were incubated for 60 min at room temperature, and the bound CK-M and CA-3 were eluted in 30% acetonitrile, 0.5% formic acid (pH ∼2.5), followed by in-solution trypsin digestion for LC/MS analysis.

LCMS/MS analysis for proteome dynamics

The LC/MS analysis was performed as previously described in detail (Shankaran *et al.* 2016*a*). The mass isotopomer distributions of peptides were measured using an Agilent 6520QToF with Chip Nano source (Agilent, Santa Clara, CA, USA). Each sample was injected twice per analysis. Mobile phase for the LC was 3% (v/v) acetonitrile, 0.1% formic acid, in 18 MΩ water (Buffer A) and 95% acetonitrile, 0.1% formic acid in 18 MΩ water (Buffer B). During the first injection, data-dependent MS–MS fragmentation spectra were collected with the instrument set to collect four MS scans per second with up to six MS–MS spectra from each scan. MS–MS fragmentation data were analysed using the Agilent software package Spectrum Mill (B0.3) and protein identifications was based on the Uniprot/Swissprot database (August 2010). The kinetic information in the mass isotopomer patterns was extracted from the MS scan data using the Mass Hunter software package (B0.4) from Agilent. The peptide list with calculated neutral mass, elemental formula and retention time was used to filter the observed isotope clusters. A visual basic application was used to calculate peptide elemental composition from lists of peptide sequences and to predict mass isotopomer patterns over a range of precursor body ^2H_2O enrichments (p) for each peptide, based on the number (n) of C–H positions in the summed amino acids in each peptide that actively incorporate ^2H from body water. Fractional synthesis rates of proteins were calculated by deconvoluting the mass isotopomer pattern of newly synthesized peptide species as compared to unlabelled species and, from this, calculating the fraction of newly synthesized peptide present, then 'rolling up' the peptides from each protein to calculate the fraction of newly synthesized protein present, as described previously (Price *et al.* 2012). The time-averaged D_2O exposure measured in each participant was used to calculate fractional synthesis for each protein at each time-point. For the second 2-week labelling period (Phase 2: ER + RT), a correction algorithm was applied by subtracting out isotopic label present in each peptide at the end of the first 2-week labelling period (Phase 1) from both the measured and the maximal labelling possible (i.e. so that the end of the initial labelling period served as a new baseline for rise-to-plateau label incorporation), in order for the additional fractional synthesis that occurred during Phase 2 to be determined.

Statistical analyses

All analyses were performed using SPSS (version 22.0, Chicago, IL, USA). Skeletal muscle mass data were analysed using a 2 × 3 (group × time) mixed-model ANOVA. Bulk MyoPS was analysed using a 2 × 2 (group × phase) mixed-model ANOVA. Muscle proteome kinetic data were analysed using a 2 × 2 (group × phase) mixed-model ANOVA; differences were considered significant with a false discovery rate of 0.2 after a Benjamini–Hochberg procedure was performed to adjust for the multiple comparisons. An in-house data analysis tool that has been developed (Shankaran *et al.* 2016*b*) was used to query and statistically analyse ontology terms of human muscle proteins, accessed programmatically from the Database for Annotation, Visualization and Integrated Discovery (DAVID) v6.8. Gene Ontology terms at high stringency of functional annotation clustering were retrieved based on an initial search of the proteins identified in the experimental datasets. The resulting terms were organized by categories (Biological Process, Cellular Component and Molecular Function) and by levels (1 to 5). Duplicate terms within categories occurring at multiple levels were filtered to include only unique ontology terms at the highest level. The mean, median, standard deviation and number of matching proteins were calculated for each ontology term, based on the corresponding proteins from experimental data. Paired two-tailed t tests with Benjamini–Hochberg multiple test corrections were then used to determine which terms were significantly enriched between experimental groups (corrected $P < 0.05$). Significant terms were then further filtered by calculating the intersection of matching proteins within each ontology term in the same category and level, removing those terms with a minimum 80% intersection with other term(s), and retaining terms with the highest number of proteins. Pearson correlation analysis was performed to correlate the FSR of CK-M and CA-3 in the muscle to that measured in the serum. Statistical significance was accepted at $P \leq 0.05$. Results are presented as means ± SD.

Results

Body composition

The change in body composition was reported previously (Murphy *et al.* 2015). Briefly, a between-group comparison was not possible due to inadequate power and groups were thus pooled for analysis. Body fat decreased over the intervention ($P < 0.001$) with no difference between phases (ER: 1.3 ± 0.2 kg, ER + RT 1.1 ± 0.2 kg; $P = 0.75$). Appendicular skeletal muscle mass (legs and arms) was unchanged in both phases (ER: −0.2 ± 0.8 kg, ER + RT: 0.0 ± 0.7 kg).

Bulk MyoPS rate

Bulk MyoPS (%/day) was similar between the BAL and SKEW groups in both the ER and the ER + RT phases. However, there was a main effect for phase ($P = 0.023$) such that bulk MyoFSR was higher during ER + RT (BAL 1.64 ± 0.48; SKEW 1.52 ± 0.66%/day) than ER (BAL 1.24 ± 0.31; SKEW 1.26 ± 0.37%/day; Fig. 2*A*). Absolute bulk MyoPS (g/day) was also greater during ER + RT (BAL 62 ± 20; SKEW 56 ± 23 g/day) than ER (BAL 47 ± 13; SKEW 47 ± 16 g/day; $P = 0.031$) with no difference between groups ($P = 0.68$; Fig. 2*B*).

Synthesis rates of individual skeletal muscle proteins

FSR data were obtained for 190 individual skeletal muscle proteins that met the criteria of being measured in both ER and ER + RT in at least two participants per group (Table 1). Mean FSRs ranged between 0.2 and 10.8%/day in ER and 0.6 and 5.5%/day in ER + RT (Table 1). FSR increased with RT in 175 of the 190 proteins with no difference between dietary groups (significant with Benjamini–Hochberg correction for multiple comparisons; Table 1). Mixed model ANOVA of FSRs of 68 proteins measured in every subject also revealed that RT increased FSR in 66 of the 68 proteins (significant with Benjamini–Hochberg correction for multiple comparisons) with no difference between dietary groups. Figure 3 shows the FSRs of several of the individual myofibrillar (*A*), sarcoplasmic (*B*) and mitochondrial (*C*) proteins that were responsive to RT.

Gene ontological analysis of muscle proteome

The mean fractional synthesis of proteins in SKEW and BAL groups in ER and ER + RT was further compared at the gene ontological level. Four non-redundant biological processes were enriched with significant differences ($P < 0.05$ in paired t tests for proteins, with Benjamini–Hochberg multiple test corrections) in mean protein FSR when comparing kinetics of the muscle proteome from participants in the SKEW *vs.* BAL groups during ER (Fig. 4). Proteins assigned to the following gene ontologies at the high stringency functional annotation clustering and the highest hierarchy level were collectively increased in the BAL group during ER, including 19 proteins involved in 'glycolytic process' (Fig. 4*A*), 5 proteins involved in 'glycogen catabolic process' (Fig. 4*B*), 32 proteins involved in 'cation transport' (Fig. 4*C*) and 64 proteins classified as being involved in 'nucleotide metabolic processes' (Fig. 4*D*); individual protein data are shown in Table 2. Gene ontological analysis comparison of protein fractional synthesis during ER + RT revealed significant differences between SKEW and BAL groups for six non-redundant biological processes at the high stringency functional annotation clustering and the highest hierarchy level (Fig. 5). The proteins that were collectively higher in the BAL group during ER + RT included 16 proteins involved in 'myofibril assembly' (Fig. 5*A*), 19 proteins involved in 'glycolytic process' (Fig. 5*B*), 34 proteins involved in 'respiratory electron transport chain' (Fig. 5*C*), 17 proteins involved in 'aerobic respiration' (Fig. 5*D*), 40 proteins involved in 'cation transport' (Fig. 5*E*) and 81 proteins involved in 'nucleotide metabolic process' (Fig. 5*F*); individual protein data are shown in Table 3.

Synthesis rates of skeletal muscle-derived proteins measured in serum

The FSR of muscle-derived proteins, CA-3 and CK-M, were measured in serum samples obtained before and

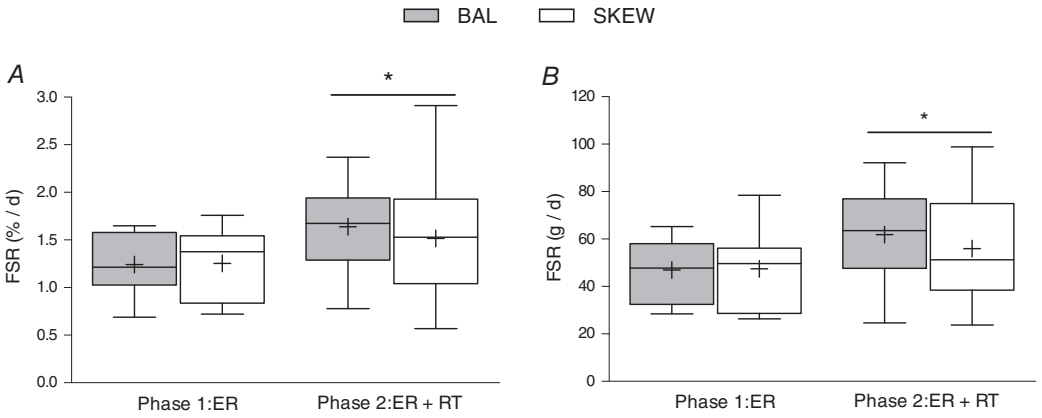

Figure 2. Relative (%/day; *A*) and absolute (g/day; *B*) myofibrillar fractional synthetic rate measured using D_2O labelling in overweight and obese older men who underwent 2 weeks of energy restriction (Phase 1: ER) and 2 weeks of energy restriction + resistance training (Phase 2: ER + RT) with balanced (BAL) or skewed (SKEW) protein distribution ($n = 10$ per group)
Data were analysed using a two-factor (group × phase) mixed-model ANOVA. *Different from Phase 1: ER; $P < 0.05$. Values are mean ± SD.

Table 1. Fractional synthetic rate (FSR) for 190 individual skeletal muscle proteins during 2 weeks of energy restriction (ER) and 2 weeks of energy plus resistance training (ER + RT)

	BAL Phase 1: ER	SKEW Phase 1: ER	BAL Phase 2: ER + RT	SKEW Phase 2: ER + RT	Benjamini–Hochberg significance
Sarcoplasmic endoplasmic reticulum calcium ATPase 1	0.98 ± 0.19 (10)	0.85 ± 0.23 (9)	2.34 ± 0.71 (10)	1.87 ± 0.66 (9)	Sig
Actin alpha skeletal muscle	0.17 ± 0.08 (10)	0.15 ± 0.09 (8)	0.70 ± 0.18 (10)	0.63 ± 0.27 (9)	Sig
Glycogen phosphorylase muscle form	0.96 ± 0.18 (10)	0.71 ± 0.20 (9)	2.11 ± 0.72 (10)	1.94 ± 0.73 (9)	Sig
Myosin-2	0.65 ± 0.25 (10)	0.70 ± 0.29 (9)	1.75 ± 0.44 (10)	1.60 ± 0.62 (9)	Sig
Sarcoplasmic endoplasmic reticulum calcium ATPase 2	0.96 ± 0.24 (10)	0.78 ± 0.15 (9)	2.45 ± 0.72 (10)	1.99 ± 0.66 (9)	Sig
Myosin-7	0.63 ± 0.31 (10)	0.80 ± 0.44 (9)	1.71 ± 0.41 (10)	1.69 ± 0.72 (9)	Sig
Creatine kinase M type	0.52 ± 0.12 (10)	0.42 ± 0.12 (9)	1.23 ± 0.39 (10)	1.13 ± 0.37 (9)	Sig
Serum albumin	2.55 ± 0.57 (10)	2.40 ± 0.49 (9)	4.20 ± 1.26 (10)	4.28 ± 1.41 (9)	Sig
Fructose bisphosphate aldolase A	0.84 ± 0.14 (10)	0.71 ± 0.17 (9)	1.89 ± 0.48 (10)	1.77 ± 0.48 (9)	Sig
Filamin C	1.71 ± 0.32 (10)	1.40 ± 0.26 (9)	3.89 ± 1.37 (10)	3.68 ± 1.40 (9)	Sig
Myosin-1	0.58 ± 0.18 (10)	0.69 ± 0.39 (8)	1.60 ± 0.43 (10)	1.46 ± 0.51 (9)	Sig
Alpha actinin-2	0.74 ± 0.13 (10)	0.69 ± 0.14 (9)	1.37 ± 0.36 (10)	1.22 ± 0.45 (9)	Sig
Myoglobin	0.58 ± 0.10 (10)	0.56 ± 0.11 (9)	0.76 ± 0.30 (10)	0.69 ± 0.18 (9)	Sig
Tropomyosin beta chain	0.52 ± 0.16 (10)	0.40 ± 0.10 (9)	1.37 ± 0.37 (10)	1.27 ± 0.41 (9)	Sig
Myosin-6	0.56 ± 0.32 (10)	0.64 ± 0.40 (9)	1.69 ± 0.41 (10)	1.65 ± 0.72 (9)	Sig
Tropomyosin alpha-1 chain	0.37 ± 0.16 (10)	0.31 ± 0.12 (9)	1.37 ± 0.42 (10)	1.22 ± 0.39 (9)	Sig
Myomesin-2	0.42 ± 0.13 (10)	0.44 ± 0.14 (8)	1.40 ± 0.26 (10)	1.43 ± 0.75 (9)	Sig
6-Phosphofructokinase, muscle type	1.39 ± 0.32 (10)	1.13 ± 0.26 (9)	3.78 ± 1.54 (10)	3.32 ± 1.15 (9)	Sig
Glycogen debranching enzyme	0.99 ± 0.11 (10)	0.74 ± 0.26 (9)	2.39 ± 0.67 (10)	2.08 ± 0.70 (9)	Sig
ATP synthase subunit beta mitochondrial	0.72 ± 0.23 (10)	0.60 ± 0.18 (9)	2.17 ± 0.80 (10)	1.84 ± 0.66 (9)	Sig
Glyceraldehyde 3 phosphate dehydrogenase	0.34 ± 0.10 (10)	0.27 ± 0.14 (9)	1.62 ± 0.40 (10)	1.33 ± 0.49 (9)	Sig
Beta-enolase	0.41 ± 0.11 (10)	0.36 ± 0.15 (8)	1.31 ± 0.37 (10)	1.23 ± 0.43 (9)	Sig
Myosin-4	0.63 ± 0.27 (10)	0.63 ± 0.35 (8)	1.53 ± 0.44 (10)	1.43 ± 0.53 (9)	Sig
Carbonic anhydrase 3	0.28 ± 0.10 (10)	0.24 ± 0.10 (9)	1.00 ± 0.39 (10)	0.86 ± 0.27 (9)	Sig
Myosin-binding protein C slow-type	2.49 ± 0.41 (10)	2.47 ± 0.71 (9)	5.09 ± 1.23 (10)	5.15 ± 1.90 (9)	Sig
Tropomyosin alpha-3 chain	0.69 ± 0.14 (10)	0.60 ± 0.25 (9)	1.52 ± 0.38 (10)	1.48 ± 0.51 (9)	Sig
Pyruvate kinase isozymes M1/M2	0.69 ± 0.20 (10)	0.60 ± 0.20 (9)	2.35 ± 0.93 (10)	2.00 ± 0.75 (9)	Sig
Myosin light chain 1/3 skeletal muscle isoform	0.27 ± 0.12 (10)	0.24 ± 0.18 (7)	0.95 ± 0.34 (10)	0.85 ± 0.35 (9)	Sig
Triosephosphate isomerase	0.33 ± 0.14 (10)	0.22 ± 0.11 (9)	1.24 ± 0.36 (10)	1.17 ± 0.43 (9)	Sig
Haemoglobin subunit beta	0.79 ± 0.20 (10)	0.55 ± 0.15 (9)	1.33 ± 0.28 (10)	1.26 ± 0.26 (9)	Sig
Myosin regulatory light chain 2 skeletal muscle isoform	0.33 ± 0.14 (10)	0.31 ± 0.18 (8)	0.98 ± 0.36 (10)	0.86 ± 0.31 (9)	Sig
Actin alpha cardiac muscle 1	0.36 ± 0.08 (10)	0.25 ± 0.14 (9)	0.65 ± 0.20 (10)	0.65 ± 0.26 (9)	Sig
Aconitate hydratase, mitochondrial	0.86 ± 0.26 (10)	0.72 ± 0.33 (9)	2.85 ± 0.95 (10)	2.67 ± 1.07 (9)	Sig
Phosphoglucomutase1	0.55 ± 0.12 (10)	0.44 ± 0.18 (9)	1.52 ± 0.57 (10)	1.38 ± 0.46 (9)	Sig
ATP synthase subunit alpha, mitochondrial	1.01 ± 0.27 (10)	0.79 ± 0.29 (9)	2.56 ± 1.02 (10)	2.14 ± 0.74 (9)	Sig
Troponin C skeletal muscle	1.76 ± 0.21 (10)	1.59 ± 0.41 (9)	3.15 ± 0.87 (10)	2.84 ± 0.68 (9)	Sig
Adenylate kinase isoenzyme 1	0.30 ± 0.09 (10)	0.30 ± 0.1 (9)	1.44 ± 0.99 (10)	0.83 ± 0.37 (9)	Sig
Creatine kinase S-type, mitochondrial	0.62 ± 0.24 (10)	0.44 ± 0.23 (9)	2.05 ± 0.71 (10)	1.72 ± 0.70 (9)	Sig
Calsequestrin-1	0.69 ± 0.24 (10)	0.59 ± 0.26 (9)	0.85 ± 0.27 (10)	0.74 ± 0.37 (9)	Sig

(*Continued*)

Table 1. Continued

	BAL Phase 1: ER	SKEW Phase 1: ER	BAL Phase 2: ER + RT	SKEW Phase 2: ER + RT	Benjamini–Hochberg significance
Glycogen phosphorylase brainform	0.98 ± 0.22 (10)	0.71 ± 0.18 (9)	2.14 ± 0.73 (10)	1.90 ± 0.68 (9)	Sig
Troponin I fast skeletal muscle	0.95 ± 0.21 (10)	0.81 ± 0.29 (9)	1.97 ± 0.51 (10)	1.76 ± 0.46 (9)	Sig
Titin	2.29 ± 1.12 (7)	1.57 ± 0.42 (8)	2.69 ± 0.77 (10)	2.63 ± 0.83 (9)	Sig
Myosin-8	0.65 ± 0.39 (9)	0.65 ± 0.35 (8)	1.58 ± 0.46 (10)	1.47 ± 0.47 (9)	Sig
Myosin-3	0.62 ± 0.24 (9)	0.78 ± 0.64 (9)	2.02 ± 0.96 (10)	1.52 ± 0.61 (9)	Sig
Phosphoglycerate kinase 1	0.26 ± 0.12 (10)	0.26 ± 0.14 (8)	1.21 ± 0.58 (10)	1.05 ± 0.46 (9)	Sig
Sarcoplasmic/endoplasmic reticulum calcium ATPase3	0.49 ± 0.20 (10)	0.35 ± 0.15 (9)	2.23 ± 0.64 (10)	1.77 ± 0.58 (9)	Sig
Myosin regulatory light chain 2, ventricular/cardiac muscle isoform	1.28 ± 0.52 (10)	1.08 ± 0.41 (9)	1.65 ± 0.66 (10)	1.67 ± 0.79 (9)	Sig
Alpha-crystallin B chain	1.40 ± 0.32 (10)	1.08 ± 0.26 (9)	3.54 ± 1.36 (10)	3.23 ± 1.05 (9)	Sig
Phosphoglycerate mutase 2	0.46 ± 0.17 (10)	0.47 ± 0.17 (9)	1.28 ± 0.37 (10)	1.16 ± 0.41 (9)	Sig
Four and a half LIM domains protein 1	1.23 ± 0.34 (10)	1.10 ± 0.53 (9)	2.07 ± 0.67 (10)	1.55 ± 0.36 (8)	Sig
ADP/ATP translocase 1	1.06 ± 0.65 (9)	0.90 ± 0.31 (8)	2.02 ± 0.53 (10)	1.76 ± 0.62 (9)	Sig
Myosin-13	0.70 ± 0.19 (10)	0.89 ± 0.84 (9)	1.50 ± 0.44 (10)	1.33 ± 0.50 (9)	Sig
Troponin T, fast skeletal muscle	0.75 ± 0.25 (10)	0.73 ± 0.24 (8)	2.28 ± 0.76 (10)	1.86 ± 0.57 (9)	Sig
Ryanodine receptor 1	2.68 ± 0.9 (9)	2.10 ± 0.47 (9)	5.34 ± 1.82 (10)	3.80 ± 1.19 (9)	Sig
Myomesin-1	1.20 ± 0.29 (9)	1.16 ± 0.39 (9)	2.38 ± 0.89 (10)	2.10 ± 0.86 (9)	Sig
Phosphatidylethanolamine-binding protein 1	0.34 ± 0.08 (8)	0.24 ± 0.17 (9)	1.21 ± 0.48 (10)	1.07 ± 0.47 (9)	Sig
Protein DJ-1	0.41 ± 0.18 (10)	0.51 ± 0.10 (9)	1.36 ± 0.91 (10)	1.11 ± 0.54 (9)	Sig
Troponin I, slow skeletal muscle	2.17 ± 0.63 (10)	1.92 ± 0.53 (9)	3.60 ± 1.11 (10)	3.37 ± 1.09 (9)	Sig
Heat shock cognate 71 kDa protein	1.30 ± 0.23 (10)	1.10 ± 0.24 (9)	3.23 ± 1.29 (10)	2.88 ± 1.17 (9)	Sig
Isocitrate dehydrogenase (NADP), mitochondrial	0.67 ± 0.29 (10)	0.44 ± 0.33 (9)	1.87 ± 0.63 (10)	1.70 ± 0.81 (9)	Sig
Heat shock protein beta-6	2.17 ± 0.46 (10)	1.84 ± 0.39 (9)	4.95 ± 1.73 (10)	4.52 ± 1.83 (9)	Sig
PDZ and LIM domain protein 3	2.49 ± 0.36 (9)	2.14 ± 0.58 (9)	4.66 ± 2.51 (10)	3.44 ± 0.99 (9)	Sig
Glucose-6 phosphate isomerase	0.31 ± 0.15 (9)	0.31 ± 0.14 (8)	1.71 ± 0.70 (10)	1.33 ± 0.70 (9)	Sig
Aspartate aminotransferase, cytoplasmic	0.50 ± 0.25 (10)	0.39 ± 0.18 (7)	1.57 ± 0.34 (10)	1.51 ± 0.44 (9)	Sig
Troponin C slow skeletal and cardiac muscles	1.92 ± 0.41 (10)	1.81 ± 0.52 (9)	3.58 ± 0.95 (10)	3.37 ± 1.35 (9)	Sig
2-Oxoglutarate dehydrogenase, mitochondrial	1.89 ± 0.45 (10)	1.60 ± 0.71 (9)	4.98 ± 2.34 (10)	4.28 ± 1.69 (9)	Sig
ATP synthase subunit b, mitochondrial	0.50 ± 0.35 (9)	0.45 ± 0.26 (9)	1.68 ± 0.74 (10)	1.22 ± 0.63 (9)	Sig
Alpha-actinin-3	0.65 ± 0.17 (10)	0.55 ± 0.11 (9)	1.44 ± 0.35 (10)	1.20 ± 0.55 (9)	Sig
Peroxiredoxin-2	0.65 ± 0.20 (10)	0.53 ± 0.21 (9)	2.03 ± 0.63 (10)	1.57 ± 0.49 (9)	Sig
Acetyl-CoA acetyltransferase, mitochondrial	0.84 ± 0.23 (10)	0.63 ± 0.29 (9)	1.88 ± 0.57 (10)	1.85 ± 0.64 (9)	Sig
Cofilin-2	0.79 ± 0.22 (10)	0.59 ± 0.19 (8)	2.26 ± 1.40 (10)	1.83 ± 0.62 (9)	Sig
ATP synthase subunit O, mitochondrial	0.50 ± 0.22 (10)	0.46 ± 0.16 (9)	1.36 ± 0.61 (10)	1.14 ± 0.49 (9)	Sig
L-Lactate dehydrogenase A chain	0.31 ± 0.19 (10)	0.24 ± 0.13 (8)	2.03 ± 0.82 (10)	1.59 ± 0.85 (9)	Sig
Cytochrome b-c1 complex subunit 2, mitochondrial	0.87 ± 0.33 (10)	0.84 ± 0.49 (9)	1.85 ± 0.53 (10)	1.80 ± 0.60 (9)	Sig
Heat shock protein beta-1	1.00 ± 0.11 (10)	0.79 ± 0.20 (9)	3.58 ± 1.72 (10)	3.11 ± 1.37 (9)	Sig
NADH-ubiquinone oxidoreductase 75 kDa subunit, mitochondrial	1.64 ± 0.57 (9)	1.62 ± 0.91 (8)	5.65 ± 2.22 (10)	5.40 ± 1.73 (9)	Sig

(*Continued*)

Table 1. Continued

	BAL Phase 1: ER	SKEW Phase 1: ER	BAL Phase 2: ER + RT	SKEW Phase 2: ER + RT	Benjamini–Hochberg significance
ATP synthase subunit d, mitochondrial	0.57 ± 0.18 (10)	0.53 ± 0.24 (9)	1.72 ± 0.80 (10)	1.36 ± 0.67 (9)	Sig
Transitional endoplasmic reticulum ATPase	3.35 ± 0.66 (9)	2.66 ± 0.49 (9)	8.79 ± 4.05 (10)	6.65 ± 2.70 (9)	Sig
Glutathione *S*-transferase Mu 2	0.81 ± 0.36 (10)	0.57 ± 0.25 (9)	1.12 ± 0.89 (10)	1.06 ± 0.52 (9)	Sig
Heat shock 70 kDa protein 1A/1B	1.34 ± 0.35 (9)	1.18 ± 0.25 (9)	3.08 ± 0.86 (10)	2.87 ± 1.21 (9)	Sig
Fructose-bisphosphate aldolase C	0.58 ± 0.20 (10)	0.52 ± 0.14 (9)	1.91 ± 0.50 (10)	1.82 ± 0.68 (9)	Sig
Puromycin-sensitive aminopeptidase	0.78 ± 0.15 (10)	0.71 ± 0.39 (9)	2.36 ± 1.19 (10)	1.87 ± 0.81 (9)	Sig
Aspartate aminotransferase, mitochondrial	0.52 ± 0.27 (10)	0.58 ± 0.31 (9)	1.25 ± 0.40 (10)	1.25 ± 0.45 (9)	Sig
Haemoglobin subunit delta	0.49 ± 0.25 (10)	0.50 ± 0.22 (7)	1.35 ± 0.33 (10)	1.27 ± 0.48 (9)	Sig
Cytochrome c oxidase subunit 4 isoform 1, mitochondrial	0.69 ± 0.49 (8)	0.74 ± 0.61 (9)	2.04 ± 0.94 (10)	1.84 ± 0.65 (9)	Sig
Alpha-actinin-1	0.90 ± 0.44 (10)	0.95 ± 0.25 (9)	1.39 ± 0.42 (10)	1.25 ± 0.62 (9)	Sig
Cytochrome b-c1 complex subunit 1, mitochondrial	0.42 ± 0.22 (9)	0.41 ± 0.27 (7)	1.98 ± 0.75 (10)	1.74 ± 0.72 (9)	Sig
Malate dehydrogenase, mitochondrial	0.76 ± 0.2 (9)	0.54 ± 0.19 (9)	1.77 ± 1.04 (10)	1.60 ± 0.82 (9)	Sig
Superoxide dismutase (Mn), mitochondrial	0.75 ± 0.26 (10)	0.60 ± 0.19 (9)	2.28 ± 0.78 (10)	1.65 ± 0.56 (9)	Sig
Sarcalumenin	0.25 ± 0.1 (7)	0.29 ± 0.17 (6)	1.92 ± 0.67 (10)	1.56 ± 0.61 (9)	Sig
Desmin	1.96 ± 0.17 (5)	1.76 ± 0.69 (2)	8.68 ± 3.76 (10)	7.70 ± 2.84 (8)	Sig
Vinculin	1.34 ± 0.32 (10)	1.28 ± 0.24 (9)	4.05 ± 1.70 (10)	3.51 ± 1.58 (9)	Sig
Ubiquitin-like modifier-activating-enzyme 1	1.44 ± 0.32 (10)	1.18 ± 0.30 (9)	3.77 ± 1.58 (10)	3.02 ± 1.22 (9)	Sig
Heat shock protein HSP 90-beta	2.14 ± 0.67 (9)	2.40 ± 1.68 (8)	15.30 ± 15.88 (10)	13.36 ± 7.80 (9)	Sig
Tripartite motif-containing protein 72	0.83 ± 0.28 (8)	0.66 ± 0.30 (6)	3.05 ± 1.35 (10)	2.77 ± 1.23 (9)	Sig
Gamma-enolase	0.19 ± 0.08 (8)	0.25 ± 0.23 (6)	1.43 ± 0.53 (10)	1.32 ± 0.58 (9)	Sig
Glutathione transferase P	0.62 ± 0.23 (10)	0.49 ± 0.12 (9)	2.22 ± 1.44 (10)	1.76 ± 0.98 (9)	Sig
Very long-chain specific acyl-CoA dehydrogenase, mitochondrial	0.76 ± 0.37 (9)	0.74 ± 0.29 (8)	3.81 ± 1.34 (10)	2.98 ± 1.2 (8)	Sig
Heat shock-related 70 kDa protein 2	1.33 ± 0.23 (10)	1.15 ± 0.23 (9)	2.99 ± 1.06 (10)	2.81 ± 1.22 (9)	Sig
Alpha-actinin-4	0.73 ± 0.16 (10)	0.72 ± 0.20 (9)	1.32 ± 0.37 (10)	1.30 ± 0.64 (9)	Sig
Mitochondrial inner membrane protein	0.65 ± 0.2 (7)	0.58 ± 0.2 (7)	2.02 ± 0.8 (10)	1.76 ± 0.76 (9)	Sig
Cytochrome b-c1 complex subunit Rieske, mitochondrial	0.87 ± 0.25 (9)	0.95 ± 0.67 (9)	3.07 ± 1.08 (10)	3.04 ± 1.44 (9)	Sig
Myosin-binding protein C, fast-type	2.12 ± 1.08 (9)	1.42 ± 0.46 (8)	4.93 ± 2.92 (10)	4.24 ± 2.10 (9)	Sig
Calcium-binding mitochondrial carrier protein Aralar1	0.66 ± 0.45 (9)	0.51 ± 0.38 (8)	2.58 ± 0.94 (10)	2.08 ± 0.95 (8)	Sig
Peroxiredoxin-1	0.96 ± 0.90 (7)	0.50 ± 0.22 (8)	2.41 ± 1.55 (10)	1.99 ± 1.30 (9)	Sig
Annexin A6	1.12 ± 0.7 (7)	0.66 ± 0.25 (4)	4.12 ± 3.44 (10)	2.68 ± 1.35 (9)	Sig
Peroxiredoxin-6	1.25 ± 0.44 (9)	1.09 ± 0.48 (8)	2.36 ± 1.34 (10)	1.59 ± 0.79 (9)	Sig
Flavin reductase (NADPH)	1.12 ± 0.40 (10)	0.89 ± 0.29 (9)	1.76 ± 0.65 (10)	1.69 ± 0.54 (9)	Sig
Ig kappa chain C region	0.84 ± 0.55 (8)	0.96 ± 0.29 (7)	3.32 ± 1.15 (10)	3.75 ± 1.08 (9)	Sig
Cytochrome c oxidase subunit 2	1.08 ± 0.31 (10)	0.84 ± 0.38 (9)	2.13 ± 0.80 (10)	1.91 ± 0.64 (9)	Sig
Thioredoxin-dependent peroxide reductase mitochondrial	0.49 ± 0.26 (9)	0.35 ± 0.19 (9)	2.60 ± 1.20 (10)	1.86 ± 0.69 (9)	Sig

(*Continued*)

Table 1. Continued

	BAL Phase 1: ER	SKEW Phase 1: ER	BAL Phase 2: ER + RT	SKEW Phase 2: ER + RT	Benjamini–Hochberg significance
Protein-arginine deiminase type-2	0.38 ± 0.32 (4)	0.56 ± 0.39 (2)	3.33 ± 2.66 (10)	2.76 ± 1.34 (9)	Sig
Fatty acid-binding protein, heart	1.03 ± 0.59 (8)	0.88 ± 0.60 (8)	1.60 ± 0.73 (10)	1.12 ± 0.72 (8)	Sig
14-3-3 Protein gamma	1.60 ± 0.27 (10)	1.48 ± 0.41 (9)	3.89 ± 1.32 (10)	3.54 ± 1.32 (9)	Sig
Dihydrolipoyl dehydrogenase, mitochondrial	1.30 ± 0.29 (9)	1.11 ± 0.41 (8)	2.60 ± 1.02 (10)	2.37 ± 0.87 (9)	Sig
Elongation factor 1-alpha 2	2.57 ± 1.90 (6)	1.82 ± 0.51 (6)	4.93 ± 2.12 (10)	3.86 ± 1.42 (8)	Sig
Heat shock protein HSP 90-alpha	4.41 ± 2.10 (3)	4.45 ± 0.87 (3)	10.02 ± 5.20 (10)	13.56 ± 9.20 (9)	Sig
Filamin-A	1.24 ± 0.3 (10)	0.81 ± 0.27 (8)	4.31 ± 1.86 (10)	4.22 ± 1.75 (9)	Sig
NADH dehydrogenase (ubiquinone) flavoprotein 2, mitochondrial	1.23 ± 0.43 (9)	1.27 ± 0.59 (9)	3.38 ± 1.39 (10)	3.92 ± 1.64 (9)	Sig
Malate dehydrogenase, cytoplasmic	0.39 ± 0.39 (10)	0.58 ± 0.7 (8)	1.47 ± 0.60 (9)	1.58 ± 0.92 (9)	Sig
Kelch-like protein 41	2.20 ± 0.56 (9)	1.64 ± 0.62 (7)	5.71 ± 3.22 (10)	5.28 ± 1.79 (8)	Sig
Glycogen starch synthase, muscle	0.94 ± 0.5 (8)	1.01 ± 0.43 (9)	4.14 ± 1.02 (10)	3.78 ± 1.26 (9)	Sig
Dihydrolipoyllysine-residue acetyltransferase component of pyruvatede dehydrogenase	0.73 (2)	0.61 ± 0.38 (4)	1.28 ± 0.53 (9)	1.17 ± 0.89 (7)	Sig
Elongation factor 2	2.16 ± 0.53 (8)	1.56 ± 0.2 (6)	5.30 ± 2.17 (8)	4.39 ± 2.09 (7)	Sig
Succinate dehydrogenase (ubiquinone) flavoprotein subunit, mitochondrial	0.90 ± 0.54 (5)	1.55 ± 0.84 (3)	3.06 ± 0.84 (10)	3.07 ± 1.07 (8)	Sig
Fructose-1,6-bisphosphatase isozyme 2	0.66 ± 0.33 (10)	0.74 ± 0.3 (8)	2.78 ± 0.94 (10)	2.97 ± 1.25 (9)	Sig
Cofilin-1	1.01 ± 0.21 (9)	0.83 ± 0.19 (8)	3.00 ± 2.54 (10)	2.32 ± 1.78 (9)	Sig
Peptidyl-prolyl *cis-trans* isomerase A	1.22 ± 0.43 (9)	1.01 ± 0.50 (8)	3.09 ± 2.18 (10)	2.48 ± 1.61 (9)	Sig
Leucine rich repeat-containing protein 20	1.98 ± 0.44 (9)	1.68 ± 0.36 (9)	2.89 ± 1.02 (10)	2.65 ± 0.72 (9)	Sig
LIM domain-binding protein 3	1.09 ± 0.54 (9)	1.07 ± 0.51 (9)	2.58 ± 0.79 (10)	2.05 ± 0.72 (9)	Sig
Glycerol-3 phosphate dehydrogenase (NAD(+)), cytoplasmic	0.55 ± 0.11 (5)	0.41 ± 0.24 (7)	1.97 ± 0.86 (10)	1.70 ± 0.90 (9)	Sig
Isochorismatase domain-containing protein 2, mitochondrial	1.37 ± 0.59 (9)	1.30 ± 0.63 (8)	3.38 ± 1.80 (9)	2.09 ± 0.60 (6)	Sig
Myomesin-3	0.53 ± 0.13 (6)	0.45 ± 0.16 (6)	1.65 ± 0.73 (10)	1.13 ± 0.67 (8)	Sig
Tubulin alpha-4A chain	2.05 ± 0.47 (5)	1.74 ± 0.68 (3)	4.54 ± 1.80 (10)	4.27 ± 2.17 (8)	Sig
1-4-3-3 Protein epsilon	1.40 ± 0.4 (10)	1.09 ± 0.49 (9)	3.89 ± 2.30 (10)	2.81 ± 1.01 (9)	Sig
Troponin T, slow skeletal muscle	0.81 ± 0.35 (10)	0.63 ± 0.42 (9)	2.73 ± 0.96 (10)	2.44 ± 1.12 (9)	Sig
Collagen alpha-3 (VI) chain	0.32 ± 0.37 (7)	0.24 ± 0.17 (3)	4.86 ± 3.80 (7)	3.92 ± 4.68 (8)	Sig
Carboxymethylenebutenolidase homologue	0.38 ± 0.21 (9)	0.34 ± 0.29 (4)	1.29 ± 0.70 (10)	1.18 ± 0.84 (8)	Sig
Glutathione *S*-transferase Mu 1	0.90 ± 0.43 (10)	0.60 ± 0.22 (7)	1.95 ± 0.78 (10)	3.22 ± 4.95 (9)	Sig
Protein-L-isoaspartate (Daspartate) *O*-methyltransferase	0.45 ± 0.15 (8)	0.21 ± 0.15 (6)	2.49 ± 0.96 (10)	1.48 ± 0.44 (7)	Sig
Citrate synthase, mitochondrial	0.76 ± 0.35 (7)	0.57 ± 0.38 (6)	1.58 ± 0.88 (10)	1.23 ± 0.72 (9)	Sig
Glutathione *S*-transferase Mu 4	0.95 ± 0.44 (8)	0.65 ± 0.30 (7)	1.95 ± 0.78 (10)	3.22 ± 4.95 (9)	Sig
Cytochrome c oxidase subunit 5A, mitochondrial	1.14 ± 0.28 (6)	0.46 ± 0.23 (8)	2.71 ± 1.14 (7)	1.80 ± 1.03 (7)	Sig
Heat shock protein beta-7	2.72 ± 0.66 (8)	2.96 ± 1.17 (7)	8.32 ± 4.21 (10)	8.44 ± 4.74 (9)	Sig
Filamin-B	2.10 ± 0.77 (6)	1.76 ± 0.29 (4)	4.21 ± 2.06 (10)	4.23 ± 1.80 (9)	Sig

(*Continued*)

Table 1. Continued

	BAL Phase 1: ER	SKEW Phase 1: ER	BAL Phase 2: ER + RT	SKEW Phase 2: ER + RT	Benjamini–Hochberg significance
Myc box-dependent-interacting protein 1	1.33 ± 0.41 (6)	1.14 ± 0.51 (5)	4.45 ± 1.51 (8)	3.67 ± 1.66 (5)	Sig
Alpha-1antitrypsin	4.72 ± 1.31 (7)	5.17 ± 0.85 (6)	12.95 ± 9.90 (9)	14.30 ± 4.71 (7)	Sig
AMP deaminase 1	0.77 ± 0.43 (4)	0.22 ± 0.17 (3)	1.48 ± 0.87 (9)	1.58 ± 0.94 (5)	Sig
GTP-binding protein SAR 1b	3.76 ± 1.21 (9)	3.19 ± 0.75 (8)	13.10 ± 12.51 (10)	8.08 ± 4.60 (8)	Sig
Glutathione *S*-transferase Mu 3	0.57 ± 0.26 (7)	0.76 ± 0.95 (6)	1.82 ± 0.66 (8)	1.15 ± 0.47 (8)	Sig
Ferritin heavy chain	2.04 ± 0.86 (8)	1.70 ± 0.92 (7)	5.74 ± 3.09 (10)	4.74 ± 2.79 (9)	Sig
Heat shock protein beta-2	0.80 ± 0.14 (9)	0.72 ± 0.31 (8)	1.93 ± 0.85 (10)	1.33 ± 0.56 (8)	Sig
Protein-cysteine *N*-palmitoyltransferase HHAT-like protein	0.43 ± 0.18 (7)	0.50 ± 0.35 (9)	0.90 ± 0.47 (10)	1.18 ± 1.10 (7)	Sig
Lumican	2.48 ± 0.62 (5)	2.22 ± 0.54 (5)	15.52 ± 11.05 (9)	7.82 ± 4.32 (6)	Sig
Proteasome subunit beta type-1	2.09 ± 0.50 (6)	1.77 ± 0.35 (6)	3.99 ± 1.93 (10)	3.26 ± 1.71 (7)	Sig
Cytochrome c1, heme protein, mitochondrial	0.29 ± 0.15 (5)	0.41 ± 0.11 (5)	1.36 ± 0.34 (9)	1.41 ± 0.65 (7)	Sig
Peroxiredoxin-5, mitochondrial	1.10 ± 0.45 (3)	0.66 ± 0.23 (6)	2.87 ± 1.1 (10)	2.67 ± 1.12 (9)	Sig
6-Phosphofructokinase, liver type	0.94 ± 0.45 (10)	0.87 ± 0.39 (8)	2.29 ± 0.88 (9)	2.09 ± 0.85 (8)	Sig
Hexokinase-1	1.15 ± 0.26 (9)	0.98 ± 0.36 (8)	3.33 ± 1.32 (9)	2.83 ± 1.20 (6)	Sig
Iggamma-1 chain C region	1.51 ± 0.07 (3)	2.34 ± 0.29 (2)	3.22 ± 1.29 (9)	3.54 ± 0.66 (8)	Sig
Translationally-controlled tumour protein	5.49 ± 2.54 (7)	3.98 ± 1.25 (8)	12.74 ± 9.23 (10)	7.24 ± 3.38 (8)	Sig
Dual specificity protein phosphatase 3	1.26 ± 0.52 (6)	0.81 ± 0.48 (8)	4.62 ± 2.1 (10)	3.61 ± 1.60 (7)	Sig
NADH dehydrogenase (ubiquinone) iron sulfur protein 7 mitochondrial	2.94 ± 0.64 (8)	2.77 ± 0.84 (8)	8.47 ± 8.36 (10)	5.76 ± 2.10 (8)	Sig
Puromycin-sensitive aminopeptidase-like protein	0.46 ± 0.21 (9)	0.31 ± 0.20 (8)	2.74 ± 0.85 (7)	2.13 ± 1.40 (6)	Sig
Short-chain specific acyl-CoA dehydrogenase, mitochondrial	1.47 ± 0.36 (5)	1.46 ± 0.79 (5)	2.01 ± 0.38 (6)	2.79 ± 1.44 (8)	Sig
Hydroxyacyl-coenzyme A dehydrogenase, mitochondrial	0.97 ± 0.11 (6)	0.58 ± 0.22 (5)	1.16 ± 0.58 (7)	0.75 ± 0.33 (6)	Sig
Collagen alpha-1 (VI) chain	0.70 ± 0.36 (6)	0.84 ± 0.45 (7)	4.62 ± 2.93 (9)	4.13 ± 5.18 (9)	Sig
Phosphorylase b kinase regulatory subunit alpha skeletal muscle isoform	1.20 ± 0.29 (6)	1.00 ± 0.33 (4)	3.08 ± 1.1 (7)	2.66 ± 1.41 (5)	Sig
SH3 domain-binding glutamic acid rich protein	1.76 ± 0.26 (8)	1.33 ± 0.33 (8)	3.32 ± 1.78 (7)	3.90 ± 2.50 (6)	Sig
Pseudouridine-5′-monophosphatase	0.52 ± 0.29 (5)	0.31 ± 0.04 (3)	1.70 ± 0.99 (9)	1.54 ± 0.43 (5)	Sig
NADH dehydrogenase (ubiquinone) 1 alpha subcomplex subunit 7	2.27 ± 1.15 (6)	1.23 ± 0.39 (5)	3.46 ± 1.97 (6)	3.42 ± 1.67 (4)	Sig
Cytochrome b5 type B	1.15 ± 0.46 (5)	1.02 ± 0.43 (5)	2.44 ± 1.10 (6)	2.94 ± 1.51 (6)	Sig
26S proteasome non- ATPase regulatory subunit 1	0.83 ± 0.17 (4)	0.63 ± 0.15 (4)	2.95 ± 1.15 (6)	2.79 ± 1.70 (5)	Sig
Adenylate kinase 2, mitochondrial	0.50 ± 0.19 (4)	0.55 ± 0.16 (2)	1.63 ± 0.90 (5)	1.09 ± 0.31 (3)	Sig
Maleylacetoacetate isomerase	0.42 ± 0.30 (4)	0.40 ± 0.29 (5)	1.27 ± 0.17 (3)	1.36 ± 0.52 (6)	Sig
Haemoglobin subunit alpha	1.16 ± 0.25 (10)	1.13 ± 0.26 (9)	1.27 ± 0.26 (10)	1.22 ± 0.32 (9)	Not sig
Apolipoprotein A-I	10.43 ± 2.66 (9)	10.21 ± 4.12 (9)	9.81 ± 5.07 (10)	14.34 ± 9.93 (9)	Not sig
Long-chain-fatty-acid-CoA ligase 1	1.19 ± 0.55 (4)	1.29 ± 1.5 (5)	1.83 ± 0.50 (10)	1.23 ± 0.72 (8)	Not sig
Superoxide dismutase (CuZn)	1.97 (2)	1.26 ± 0.67 (3)	1.69 ± 0.97 (10)	1.22 ± 0.68 (9)	Not sig

(*Continued*)

Table 1. Continued

	BAL Phase 1: ER	SKEW Phase 1: ER	BAL Phase 2: ER + RT	SKEW Phase 2: ER + RT	Benjamini–Hochberg significance
Pyruvate dehydrogenase E1 component subunit alpha, somatic form mitochondrial	2.04 ± 1.36 (8)	1.58 ± 0.65 (8)	2.18 ± 0.75 (10)	1.81 ± 0.82 (9)	Not sig
Polyubiquitin-C	10.78 ± 3.09 (7)	8.01 ± 2.10 (7)	9.77 ± 6.02 (8)	12.66 ± 10.68 (7)	Not sig
Reticulon-2	1.03 ± 0.14 (6)	1.18 ± 0.41 (9)	2.13 ± 0.90 (10)	1.34 ± 0.90 (9)	Not sig
Nucleoside diphosphate kinase B	1.84 ± 0.76 (6)	0.76 ± 0.12 (4)	2.19 ± 1.18 (9)	2.22 ± 1.99 (8)	Not sig
NADH dehydrogenase (ubiquinone) 1 beta subcomplex subunit 9	1.16 ± 0.76 (8)	0.58 ± 0.37 (5)	1.25 ± 0.47 (8)	1.26 ± 0.48 (6)	Not sig
Nucleoside diphosphate kinase A	1.84 ± 0.76 (6)	0.76 ± 0.12 (4)	1.60 ± 0.64 (7)	2.21 ± 2.00 (8)	Not sig
Ras-related protein Rab-7a	1.24 ± 0.36 (5)	1.15 ± 0.36 (8)	11.39 ± 8.63 (8)	6.32 ± 4.30 (6)	Not sig
NADH dehydrogenase (ubiquinone) 1 alpha subcomplex subunit 13	0.38 ± 0.28 (2)	0.52 ± 0.42 (4)	1.68 ± 0.87 (8)	0.62 ± 0.47 (3)	Not sig
ATP synthase subunit g, mitochondrial	0.98 ± 0.24 (5)	0.88 ± 0.57 (6)	1.50 ± 0.59 (3)	0.59 ± 0.25 (4)	Not sig
Cytochrome c oxidase subunit 6B1	0.83 ± 0.79 (2)	0.26 ± 0.18 (2)	2.08 ± 1.49 (3)	1.80 ± 0.76 (5)	Not sig
NADH-dehydrogenase (ubiquinone) 1 alpha subcomplex subunit 5	3.00 ± 0.47 (2)	2.03 ± 0.66 (4)	3.06 ± 1.75 (3)	2.70 ± 2.06 (2)	Not sig

Values are means ± SD (*n*). FSR, fractional synthetic rate (%/day); ER, energy restriction; ER + RT, energy restriction plus resistance training. Sig, significance according to Benjamini–Hochberg procedure to adjust for the multiple comparisons with a false discovery rate of 0.2.

after RT in the SKEW and BAL groups. In both SKEW and BAL groups, there was an increase in FSR of serum CA-3 ($P < 0.001$ main effect for phase, $P < 0.05$ in SKEW, $P < 0.001$ in BAL, Fig. 6*A*) and CK-M ($P < 0.001$ main effect for phase, $P < 0.05$ in SKEW, $P < 0.005$ in BAL, Fig. 6*B*) during ER + RT compared to ER alone. The serum CA-3 and CK-M FSRs were similar in BAL and SKEW. Significant correlations between serum CA-3 and muscle CA-3 FSR ($r = 0.6527$, $P < 0.0001$, Fig. 6*C*) as well as between serum CK-M FSR and muscle CK-M FSR ($r = 0.5733$, $P < 0.0005$, Fig. 6*D*) were observed. In addition, both serum CK-M FSR and serum CA-3 FSR correlated significantly with FSR of myofibrillar proteins such as actin ($r = 0.5875$, $P = 0.0001$, Fig. 7*A*; $r = 0.6239$, $P < 0.0001$, Fig. 7*B*), myosin ($r = 0.5895$, $P < 0.0001$, Fig. 7*C*; $r = 0.6517$, $P < 0.0001$, Fig. 7*D*), tropomyosin ($r = 0.6236$, $P < 0.0001$, Fig. 7*E*; $r = 0.6127$, $P < 0.0001$, Fig. 7*F*) and troponin ($r = 0.6179$, $P < 0.0001$, Fig. 7*G*; $r = 0.5997$, $P < 0.0001$, Fig. 7*H*).

MyoPS: comparison of D_2O and L-[ring-$^{13}C_6$]-phenylalanine tracers

Table 4 provides a comparison between bulk MyoPS rates measured via D_2O in the current study and the rates measured acutely via L-[ring-$^{13}C_6$]-phenylalanine ($^{13}C_6$ Phe) infusion in the same participants in our previous study (Murphy *et al.* 2015). A Bland–Altman plot of the agreement between the two approaches is shown in Fig. 8. The calculated bias between the free-living (D_2O) and laboratory-based ($^{13}C_6$ Phe) rates is −0.5048%/day (limits of agreement: −1.430, 0.4201). Proportional bias can be observed such that as the average of the MyoPS rates increase the difference between the free-living (D_2O) and laboratory-based ($^{13}C_6$ Phe) rates becomes larger.

Discussion

We used the D_2O labelling approach combined with tandem mass spectrometric analysis of proteins across the proteome (Shankaran *et al.* 2016*a*) to estimate the bulk MyoPS and the synthesis rates of individual skeletal muscle proteins over 2 week of ER and 2 week of ER + RT in overweight/obese older men who consumed their dietary protein in either a balanced or a skewed pattern. This extends our previous work (Murphy *et al.* 2015) which showed that a balanced distribution of dietary protein ingestion more effectively stimulated MyoPS over an 11 h period *versus* a skewed distribution in overweight and obese older men during ER, both with and without RT. In contrast to an acute (i.e. 11 h) labelling period and contrary to our original hypothesis, we found little influence of the distribution of daily protein on integrative (i.e. 2-week) bulk MyoPS during our intervention. However, a subtle

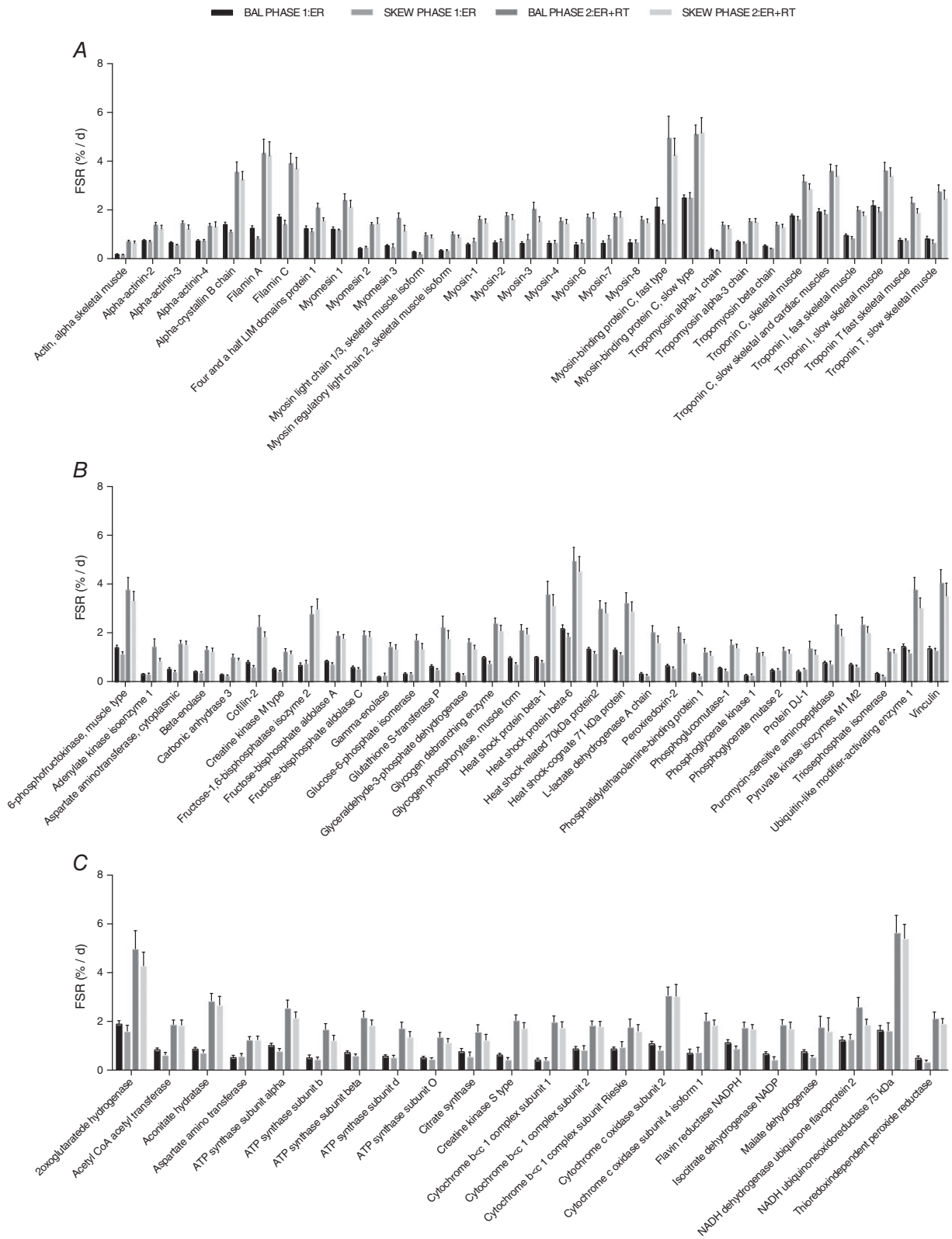

Figure 3. Fractional synthetic rate (FSR) of selected individual myofibrillar (*A*), sarcoplasmic (*B*) and mitochondrial (*C*) proteins in overweight and obese older men who underwent 2 weeks of energy restriction (Phase 1: ER) and 2 weeks of energy restriction + resistance training (Phase 2: ER + RT) with balanced (BAL) or skewed (SKEW) protein distribution

FSRs for all proteins shown were higher during Phase 2: ER + RT than during Phase 1: ER with no differences between groups. Proteome kinetic data were analysed using a 2 × 2 (group × phase) mixed-model ANOVA, and differences were considered significant with a false discovery rate of 0.2 after a Benjamini–Hochberg procedure was performed to adjust for the multiple comparisons. Values are mean ± SEM.

effect of the dietary protein distribution was revealed by gene ontological analysis of proteome dynamics, wherein participants in the BAL group had a higher rate of synthesis of proteins involved in several metabolic processes during ER, and increased synthesis of several metabolic and structural proteins during ER + RT compared to the SKEW group. Moreover, in agreement with our previous data, integrative bulk MyoPS and the synthetic rates of most individual myofibrillar, sarcoplasmic and mitochondrial proteins measured across many gene ontologies were higher in ER + RT compared to ER alone. In addition, rates of skeletal muscle-derived (synthesized) proteins measured in serum samples (CK-M and CA-3) mirrored the synthetic rates of numerous skeletal muscle proteins obtained via muscle biopsies.

The observation of little influence of the distribution of daily protein on the longer-term integrative MyoPS (%/day) response contrasts with our earlier work showing that a balanced distribution (3 × 25 g evenly spaced doses of protein) *versus* a skewed distribution of the same amount of protein (10 g at breakfast, 15 g at lunch, 50 g at dinner) stimulated bulk MyoPS more effectively over 11 h during ER (Murphy *et al.* 2015) measured using the primed, continuous intravenous infusion of an isotopically labelled amino acid (i.e. $^{13}C_6$ Phe). In the present study (which was conducted in the same participants as our previous study) we used the oral administration of D_2O. When used simultaneously, these methods have been reported to yield comparable mean MyoPS rates measured over several hours (Wilkinson *et al.* 2015). As such, it appears unlikely that differences in the validity of the two methods per se account for the inconsistency between our acute and longer-term findings. A more likely explanation for the discrepancy

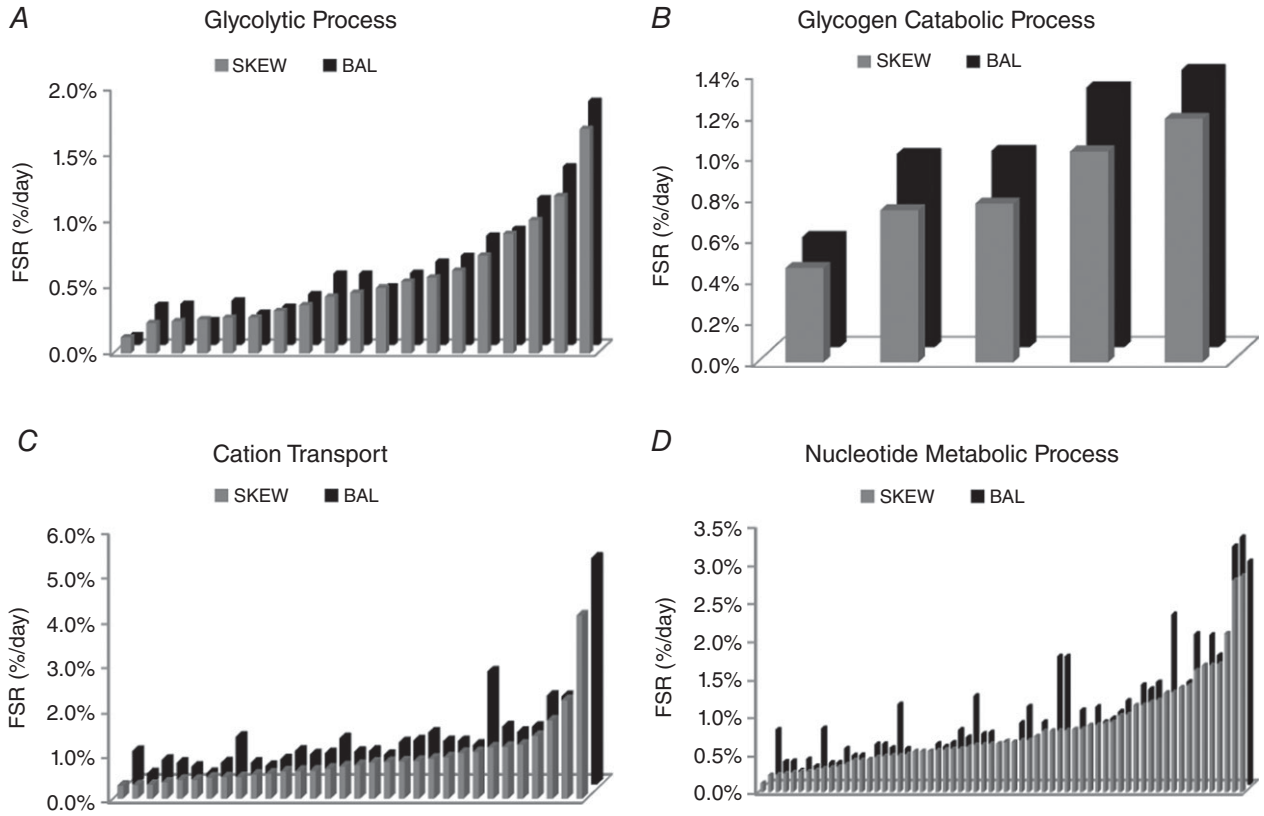

Figure 4. Mean fractional synthesis of proteins in DAVID gene ontology terms, biological processes level 5, that were significantly different as a group ($P < 0.05$ in paired *t* tests for proteins with Benjamini–Hochberg multiple test corrections) in participants who consumed a balanced (BAL) or skewed (SKEW) protein distribution during 2 weeks of energy restriction (Phase 1)
Each bar represents the mean fractional synthetic rate (FSR) of a protein within the DAVID gene ontology term. Names and data for the proteins are provided in Table 2.

Table 2. Mean FSR (% per day) of proteins in DAVID gene ontology terms that were significantly different as a group ($P < 0.05$ after Benjamini–Hochberg correction for multiple comparisons) in SKEW *vs*. BAL during 2 weeks of energy restriction (ER)

Gene Ontology term: Biological Process Level 5	Accession number	Protein name	SKEW mean FSR (%/day)	BAL mean FSR (%/day)
Glycolytic process GO:0006096, 19 proteins				
	P06733	Alpha-enolase	0.12%	0.08%
	P60174	Triosephosphate isomerase	0.23%	0.30%
	P00338	L-Lactate dehydrogenase A chain	0.24%	0.31%
	P09104	Gamma-enolase	0.26%	0.19%
	P04406	Glyceraldehyde-3-phosphate dehydrogenase	0.27%	0.34%
	P00558	Phosphoglycerate kinase 1	0.27%	0.25%
	P06744	Glucose-6-phosphate isomerase	0.32%	0.29%
	P13929	Beta-enolase	0.36%	0.39%
	P21695	Glycerol-3-phosphate dehydrogenase [NAD(+)], cytoplasmic	0.43%	0.54%
	P36871	Phosphoglucomutase-1	0.46%	0.54%
	P15259	Phosphoglycerate mutase 2	0.50%	0.44%
	P09972	Fructose-bisphosphate aldolase C	0.54%	0.54%
	Q08043	Alpha-actinin-3	0.57%	0.63%
	P14618	Pyruvate kinase isozymes M1/M2	0.62%	0.67%
	P04075	Fructose-bisphosphate aldolase A	0.74%	0.83%
	P17858	6-phosphofructokinase, liver type	0.90%	0.88%
	P19367	Hexokinase-1	1.00%	1.11%
	P08237	6-Phosphofructokinase, muscle type	1.19%	1.35%
	Q02218	2-Oxoglutarate dehydrogenase, mitochondrial	1.69%	1.84%
Glycogen catabolic process GO:0005980, 5 proteins				
	P36871	Phosphoglucomutase-1	0.46%	0.54%
	P11217	Glycogen phosphorylase, muscle form	0.74%	0.94%
	P35573	Glycogen debranching enzyme	0.77%	0.96%
	P46020	Phosphorylase b kinase regulatory subunit alpha, skeletal muscle isoform	1.03%	1.26%
	P08237	6-Phosphofructokinase, muscle type	1.19%	1.35%
Cation transport GO:006812, 32 proteins				
	P14854	Cytochrome c oxidase subunit 6B1	0.29%	0.74%
	Q86TD4	Sarcalumenin	0.30%	0.24%
	P21796	Voltage-dependent anion-selective channel protein 1	0.31%	0.54%
	Q93084	Sarcoplasmic/endoplasmic reticulum calcium ATPase 3	0.36%	0.48%
	P31930	Cytochrome b-c1 complex subunit 1, mitochondrial	0.42%	0.39%
	P08574	Cytochrome c1, heme protein, mitochondrial	0.42%	0.25%
	P24539	ATP synthase subunit b, mitochondrial	0.47%	0.49%
	P20674	Cytochrome c oxidase subunit 5A, mitochondrial	0.48%	1.06%
	P48047	ATP synthase subunit O, mitochondrial	0.48%	0.48%
	Q99497	Protein DJ-1	0.54%	0.41%
	O75947	ATP synthase subunit d, mitochondrial	0.56%	0.56%
	P28161	Glutathione *S*-transferase Mu 2	0.61%	0.75%
	P31415	Calsequestrin-1	0.62%	0.67%
	P06576	ATP synthase subunit beta, mitochondrial	0.63%	0.69%
	P08133	Annexin A6	0.67%	1.03%
	P35609	Alpha-actinin-2	0.72%	0.72%
	O43707	Alpha-actinin-4	0.75%	0.75%
	P13073	Cytochrome c oxidase subunit 4 isoform 1, mitochondrial	0.80%	0.66%
	P16615	Sarcoplasmic/endoplasmic reticulum calcium ATPase 2	0.82%	0.94%
	P25705	ATP synthase subunit alpha, mitochondrial	0.83%	0.98%
	P21333	Filamin-A	0.84%	1.16%

(*Continued*)

Table 2. Continued

Gene Ontology term: Biological Process Level 5	Accession number	Protein name	SKEW mean FSR (%/day)	BAL mean FSR (%/day)
	O14983	Sarcoplasmic/endoplasmic reticulum calcium ATPase 1	0.89%	0.96%
	O75964	ATP synthase subunit g, mitochondrial	0.92%	0.96%
	P47985	Cytochrome b-c1 complex subunit Rieske, mitochondrial	1.02%	0.88%
	P23297	Protein S100-A1	1.04%	2.52%
	P62258	14-3-3 Protein epsilon	1.15%	1.30%
	Q13642	Four and a half LIM domains protein 1	1.15%	1.17%
	P54652	Heat shock-related 70 kDa protein 2	1.20%	1.29%
	P14927	Cytochrome b-c1 complex subunit 7	1.40%	1.98%
	P02794	Ferritin heavy chain	1.75%	1.98%
	P21817	Ryanodine receptor 1	2.21%	2.61%
	P13693	Translationally controlled tumour protein	4.10%	5.07%
Nucleotide metabolic process GO:0009117, 64 proteins				
	P06733	Alpha-enolase	0.12%	0.08%
	P23109	AMP deaminase 1	0.22%	0.73%
	P60174	Triosephosphate isomerase	0.23%	0.30%
	P00338	L-Lactate dehydrogenase A chain	0.24%	0.31%
	P09104	Gamma-enolase	0.26%	0.19%
	P04406	Glyceraldehyde-3-phosphate dehydrogenase	0.27%	0.34%
	P00558	Phosphoglycerate kinase 1	0.27%	0.25%
	P14854	Cytochrome c oxidase subunit 6B1	0.29%	0.74%
	P00568	Adenylate kinase isoenzyme 1	0.31%	0.29%
	P06744	Glucose-6-phosphate isomerase	0.32%	0.29%
	Q08623	Pseudouridine-5′-monophosphatase	0.33%	0.48%
	P13929	Beta-enolase	0.36%	0.39%
	P31930	Cytochrome b-c1 complex subunit 1, mitochondrial	0.42%	0.39%
	P08574	Cytochrome c1, heme protein, mitochondrial	0.42%	0.25%
	P21695	Glycerol-3-phosphate dehydrogenase [NAD(+)], cytoplasmic	0.43%	0.54%
	P36871	Phosphoglucomutase-1	0.46%	0.54%
	P24539	ATP synthase subunit b, mitochondrial	0.47%	0.49%
	P20674	Cytochrome c oxidase subunit 5A, mitochondrial	0.48%	1.06%
	P48047	ATP synthase subunit O, mitochondrial	0.48%	0.48%
	P15259	Phosphoglycerate mutase 2	0.50%	0.44%
	Q99497	Protein DJ-1	0.54%	0.41%
	Q9P0J0	NADH dehydrogenase [ubiquinone] 1 alpha subcomplex subunit 13	0.54%	0.40%
	P09972	Fructose-bisphosphate aldolase C	0.54%	0.54%
	P54819	Adenylate kinase 2, mitochondrial	0.55%	0.51%
	O75947	ATP synthase subunit d, mitochondrial	0.56%	0.56%
	P40926	Malate dehydrogenase, mitochondrial	0.56%	0.72%
	Q08043	Alpha-actinin-3	0.57%	0.63%
	Q9Y6M9	NADH dehydrogenase [ubiquinone] 1 Beta subcomplex subunit 9	0.59%	1.17%
	P14618	Pyruvate kinase isozymes M1/M2	0.62%	0.67%
	P06576	ATP synthase subunit beta, mitochondrial	0.63%	0.69%
	P40925	Malate dehydrogenase, cytoplasmic	0.64%	0.36%
	Q9Y623	Myosin-4	0.64%	0.57%
	P13533	Myosin-6	0.66%	0.53%
	P24752	Acetyl-CoA acetyltransferase, mitochondrial	0.66%	0.81%
	P30044	Peroxiredoxin-5, mitochondrial	0.68%	1.03%
	P13535	Myosin-8	0.68%	0.63%
	P04075	Fructose-bisphosphate aldolase A	0.74%	0.83%

(*Continued*)

Table 2. Continued

Gene Ontology term: Biological Process Level 5	Accession number	Protein name	SKEW mean FSR (%/day)	BAL mean FSR (%/day)
	P13073	Cytochrome c oxidase subunit 4 isoform 1, mitochondrial	0.80%	0.66%
	P15531	Nucleoside diphosphate kinase A	0.81%	1.69%
	P22392	Nucleoside diphosphate kinase B	0.81%	1.69%
	P11055	Myosin-3	0.82%	0.56%
	P25705	ATP synthase subunit alpha, mitochondrial	0.83%	0.98%
	P12883	Myosin-7	0.83%	0.60%
	P00403	Cytochrome c oxidase subunit 2	0.88%	1.03%
	P22695	Cytochrome b-c1 complex subunit 2, mitochondrial	0.88%	0.83%
	P17858	6-Phosphofructokinase, liver type	0.90%	0.88%
	O75964	ATP synthase subunit g, mitochondrial	0.92%	0.96%
	P19367	Hexokinase-1	1.00%	1.11%
	P47985	Cytochrome b-c1 complex subunit Rieske, mitochondrial	1.02%	0.88%
	P09622	Dihydrolipoyl dehydrogenase, mitochondrial	1.14%	1.31%
	P11142	Heat shock cognate 71 kDa protein	1.15%	1.26%
	P08237	6-Phosphofructokinase, muscle type	1.19%	1.35%
	P30085	UMP-CMP kinase	1.21%	0.78%
	O95182	NADH dehydrogenase [ubiquinone] 1 alpha subcomplex subunit 7	1.31%	2.24%
	P19404	NADH dehydrogenase [ubiquinone] flavoprotein 2, mitochondrial	1.32%	1.19%
	P49773	Histidine triad nucleotide-binding protein 1	1.38%	1.35%
	P14927	Cytochrome b-c1 complex subunit 7	1.40%	1.98%
	P31040	Succinate dehydrogenase [ubiquinone] flavoprotein subunit, mitochondrial	1.60%	1.05%
	P08559	Pyruvate dehydrogenase E1 component subunit alpha, somatic form, mitochondrial	1.67%	1.97%
	P28331	NADH-ubiquinone oxidoreductase 75 kDa subunit, mitochondrial	1.67%	1.71%
	Q02218	2-Oxoglutarate dehydrogenase, mitochondrial	1.69%	1.84%
	Q16718	NADH dehydrogenase [ubiquinone] 1 alpha subcomplex subunit 5	2.08%	3.14%
	P55072	Transitional endoplasmic reticulum ATPase	2.79%	3.26%
	O75251	NADH dehydrogenase [ubiquinone] iron-sulfur protein 7, mitochondrial	2.84%	2.94%

is the conditions under which MPS measurements were conducted. The continuous labelled amino acid infusion technique provides sensitive measurements of MPS under controlled laboratory conditions and is most suitable for assessing the acute response (2–24 h) to specific stimuli such as feeding or exercise (Rennie *et al.* 1994). As such, this approach may be more sensitive to detecting subtle effects of dietary protein intake pattern on MPS. Nevertheless, this technique restricts the acquisition of long-term, potentially more relevant, measures of muscle in free-living settings. Here we report on longer-term bulk MyoPS (%/day) measured over a 2-week free-living period in which several variables could potentially have modified MyoPS (i.e. timing and consumption of prescribed meals, variability in activities of daily living, daily stresses and/or sleep duration). Moreover, an important finding from our acute study was that the influence of protein distribution on bulk MyoPS was specific to the fed and not the fasted rates of MyoPS (Murphy *et al.* 2015); thus, fasted periods, particularly the extended overnight fast, may have 'diluted' feeding-specific effects on MyoPS. Additionally, in our previous work (Murphy *et al.* 2015), protein was consumed as isolated whey protein in liquid form whereas dietary protein was mainly provided in mixed macronutrient meals in the current study protocol. The achievement of a rapid and pronounced increase in plasma indispensible amino acid/leucine concentrations, which is characteristic of whey protein ingestion, is associated

with increased rates of MyoPS compared to a slow rate of appearance of these amino acids (West *et al.* 2011). Consumption of solid food and co-ingestion of other nutrients (carbohydrate, fat and dietary fibre) modifies amino acid digestion and absorption kinetics and blunts postprandial aminoacidaemia/leucinaemia (Conley *et al.* 2011; Burke *et al.* 2012). As such, it remains possible that the consumption of a given protein dose within a solid, mixed macronutrient meal may attenuate the MPS response.

When extrapolated to %/day, the acute rates of MyoPS measured in the laboratory setting (Murphy *et al.* 2015) were lower than those obtained using D_2O (Table 4, Fig. 8). Of relevance here is that for the duration of the acute

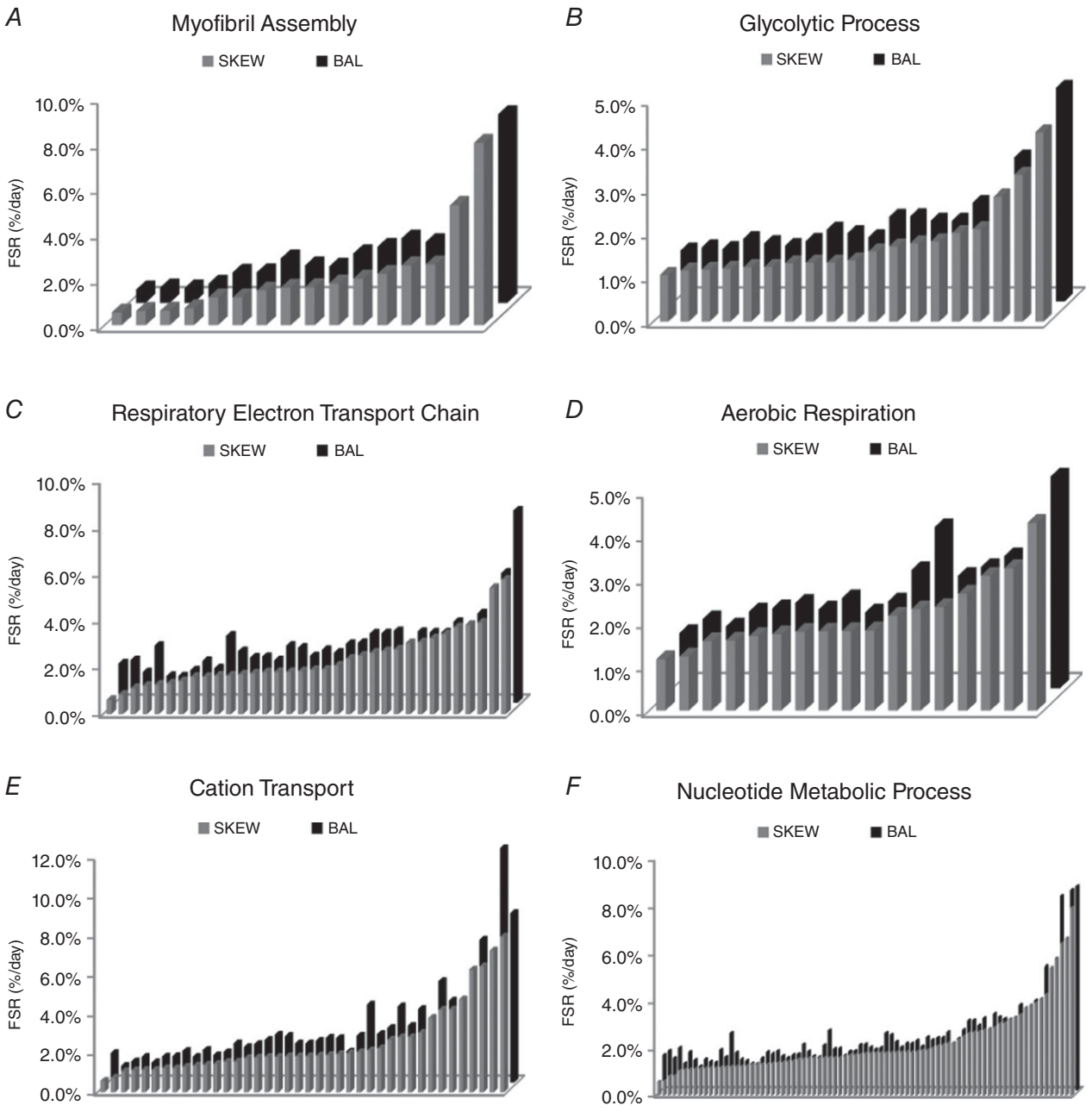

Figure 5. Mean FSR of proteins in DAVID gene ontology terms, biological processes level 5, that were significantly different as a group ($P < 0.05$ in paired t tests for proteins with Benjamini–Hochberg multiple test corrections) in participants who consumed a balanced (BAL) or skewed (SKEW) protein distribution during 2 weeks of energy restriction + resistance training (Phase 2)
Each bar represents the mean fractional synthetic rate (FSR) of a protein within the DAVID gene ontology term. Names and data for the proteins are provided in Table 3.

Table 3. Mean FSR (%/day) of proteins in DAVID gene ontology terms that were significantly different as a group ($P < 0.05$ after Benjamini–Hochberg correction for multiple comparisons) in SKEW *vs*. BAL during 2 weeks of energy restriction plus resistance training (ER + RT)

Gene ontology term: Biological Process Level 5	Accession number	Protein name	SKEW mean FSR (%/day)	BAL mean FSR (%/day)
Myofibril Assembly GO:0030239, 16 proteins				
	P63261	Actin, cytoplasmic 2	0.56%	0.59%
	P68133	Actin, alpha skeletal muscle	0.63%	0.68%
	P68032	Actin, alpha cardiac muscle 1	0.65%	0.64%
	P31415	Calsequestrin-1	0.74%	0.84%
	P09493	Tropomyosin alpha-1 chain	1.22%	1.32%
	P35609	Alpha-actinin-2	1.22%	1.34%
	P11055	Myosin-3	1.52%	1.95%
	P13533	Myosin-6	1.65%	1.64%
	P10916	Myosin regulatory light chain 2, ventricular/cardiac muscle isoform	1.67%	1.59%
	Q9Y281	Cofilin-2	1.83%	2.18%
	O75112	LIM domain-binding protein 3	2.05%	2.45%
	O75083	WD repeat-containing protein 1	2.26%	2.83%
	Q8WZ42	Titin	2.63%	2.66%
	P10644	cAMP-dependent protein kinase type I-alpha regulatory subunit	2.67%	3.84%
	O60662	Kelch-like protein 41	5.28%	5.44%
	Q5VST9	Obscurin	8.00%	8.27%
Glycolytic process GO:0006096, 19 proteins				
	P00558	Phosphoglycerate kinase 1	1.05%	1.16%
	P15259	Phosphoglycerate mutase 2	1.16%	1.23%
	P60174	Triosephosphate isomerase	1.17%	1.19%
	Q08043	Alpha-actinin-3	1.20%	1.41%
	P06733	Alpha-enolase	1.23%	1.32%
	P13929	Beta-enolase	1.23%	1.26%
	P09104	Gamma-enolase	1.32%	1.37%
	P06744	Glucose-6-phosphate isomerase	1.33%	1.63%
	P04406	Glyceraldehyde-3-phosphate dehydrogenase	1.33%	1.55%
	P36871	Phosphoglucomutase-1	1.38%	1.45%
	P21695	Glycerol-3-phosphate dehydrogenase [NAD(+)], cytoplasmic	1.70%	1.93%
	P04075	Fructose-bisphosphate aldolase A	1.77%	1.83%
	P09972	Fructose-bisphosphate aldolase C	1.82%	1.83%
	P14618	Pyruvate kinase isozymes M1/M2	2.00%	2.23%
	P17858	6-Phosphofructokinase, liver type	2.09%	2.23%
	P19367	Hexokinase-1	2.83%	3.25%
	P08237	6-Phosphofructokinase, muscle type	3.32%	3.63%
	Q02218	2-Oxoglutarate dehydrogenase, mitochondrial	4.28%	4.83%
Respiratory Electron Transport Chain GO:0022904, 34 proteins				
	Q9P0J0	NADH dehydrogenase [ubiquinone] 1 alpha subcomplex subunit 13	0.62%	1.68%
	O95169	NADH dehydrogenase [ubiquinone] 1 beta subcomplex subunit 8, mitochondrial	0.84%	1.81%
	Q99497	Protein DJ-1	1.11%	1.30%
	P99999	Cytochrome c	1.21%	2.43%
	Q9Y6M9	NADH dehydrogenase [ubiquinone] 1 beta subcomplex subunit 9	1.26%	1.14%
	O96000	NADH dehydrogenase [ubiquinone] 1 beta subcomplex subunit 10	1.31%	1.13%

(*Continued*)

Table 3. Continued

Gene ontology term: Biological Process Level 5	Accession number	Protein name	SKEW mean FSR (%/day)	BAL mean FSR (%/day)
	P08574	Cytochrome c1, heme protein, mitochondrial	1.41%	1.38%
	P03905	NADH-ubiquinone oxidoreductase chain 4	1.60%	1.78%
	O43674	NADH dehydrogenase [ubiquinone] 1 beta subcomplex subunit 5, mitochondrial	1.60%	1.47%
	P51649	Succinate-semialdehyde dehydrogenase, mitochondrial	1.65%	2.87%
	P04179	Superoxide dismutase [Mn], mitochondrial	1.65%	2.20%
	P21695	Glycerol-3-phosphate dehydrogenase [NAD(+)], cytoplasmic	1.70%	1.93%
	P31930	Cytochrome b-c1 complex subunit 1, mitochondrial	1.74%	1.95%
	P22695	Cytochrome b-c1 complex subunit 2, mitochondrial	1.80%	1.81%
	P20674	Cytochrome c oxidase subunit 5A, mitochondrial	1.80%	2.43%
	P14854	Cytochrome c oxidase subunit 6B1	1.80%	2.36%
	P13073	Cytochrome c oxidase subunit 4 isoform 1, mitochondrial	1.84%	1.99%
	P10606	Cytochrome c oxidase subunit 5B, mitochondrial	1.90%	2.26%
	P00403	Cytochrome c oxidase subunit 2	1.91%	2.14%
	O75746	Calcium-binding mitochondrial carrier protein Aralar1	2.08%	2.52%
	P09622	Dihydrolipoyl dehydrogenase, mitochondrial	2.37%	2.56%
	O75489	NADH dehydrogenase [ubiquinone] iron-sulfur protein 3, mitochondrial	2.50%	2.96%
	Q9UI09	NADH dehydrogenase [ubiquinone] 1 alpha subcomplex subunit 12	2.63%	2.98%
	Q16718	NADH dehydrogenase [ubiquinone] 1 alpha subcomplex subunit 5	2.70%	3.06%
	O95168	NADH dehydrogenase [ubiquinone] 1 beta subcomplex subunit 4	2.77%	2.10%
	P47985	Cytochrome b-c1 complex subunit Rieske, mitochondrial	3.04%	3.04%
	P31040	Succinate dehydrogenase [ubiquinone] flavoprotein subunit, mitochondrial	3.07%	3.01%
	P49821	NADH dehydrogenase [ubiquinone] flavoprotein 1, mitochondrial	3.24%	3.01%
	O95182	NADH dehydrogenase [ubiquinone] 1 alpha subcomplex subunit 7	3.42%	3.46%
	O00217	NADH dehydrogenase [ubiquinone] iron-sulfur protein 8, mitochondrial	3.72%	3.18%
	O75306	NADH dehydrogenase [ubiquinone] iron-sulfur protein 2, mitochondrial	3.82%	3.82%
	P19404	NADH dehydrogenase [ubiquinone] flavoprotein 2, mitochondrial	3.92%	3.36%
	P28331	NADH-ubiquinone oxidoreductase 75 kDa subunit, mitochondrial	5.40%	5.56%
	O75251	NADH dehydrogenase [ubiquinone] iron-sulfur protein 7, mitochondrial	5.76%	8.23%
Aerobic Respiration GO:0009060, 17 proteins				
	P10515	Dihydrolipoyllysine-residue acetyltransferase component of pyruvate dehydrogenase complex, mitochondrial	1.17%	1.26%

(*Continued*)

Table 3. Continued

Gene ontology term: Biological Process Level 5	Accession number	Protein name	SKEW mean FSR (%/day)	BAL mean FSR (%/day)
	O75390	Citrate synthase, mitochondrial	1.23%	1.58%
	P40925	Malate dehydrogenase, cytoplasmic	1.58%	1.41%
	P40926	Malate dehydrogenase, mitochondrial	1.60%	1.76%
	P48735	Isocitrate dehydrogenase [NADP], mitochondrial	1.70%	1.83%
	P31930	Cytochrome b-c1 complex subunit 1, mitochondrial	1.74%	1.95%
	P22695	Cytochrome b-c1 complex subunit 2, mitochondrial	1.80%	1.81%
	P08559	Pyruvate dehydrogenase E1 component subunit alpha, somatic form, mitochondrial	1.81%	2.06%
	P36957	Dihydrolipoyllysine-residue succinyltransferase component of 2-oxoglutarate dehydrogenase complex, mitochondrial	1.81%	1.74%
	Q13423	NAD(P) transhydrogenase, mitochondrial	1.83%	1.99%
	P07954	Fumarate hydratase, mitochondrial	2.16%	2.70%
	Q9P2R7	Succinyl-CoA ligase [ADP- forming] subunit beta, mitochondrial	2.31%	3.67%
	P09622	Dihydrolipoyl dehydrogenase, mitochondrial	2.37%	2.56%
	Q99798	Aconitate hydratase, mitochondrial	2.67%	2.76%
	P31040	Succinate dehydrogenase [ubiquinone] flavoprotein subunit, mitochondrial	3.07%	3.01%
	P49821	NADH dehydrogenase [ubiquinone] flavoprotein 1, mitochondrial	3.24%	3.01%
	Q02218	2-Oxoglutarate dehydrogenase, mitochondrial	4.28%	4.83%
Cation Transport GO:0066812, 42 proteins				
	O75964	ATP synthase subunit g, mitochondrial	0.59%	1.50%
	P31415	Calsequestrin-1	0.74%	0.84%
	P28161	Glutathione *S*-transferase Mu 2	1.06%	1.07%
	Q99497	Protein DJ-1	1.11%	1.30%
	P30049	ATP synthase subunit delta, mitochondrial	1.14%	1.03%
	P48047	ATP synthase subunit O, mitochondrial	1.14%	1.32%
	P35609	Alpha-actinin-2	1.22%	1.34%
	P24539	ATP synthase subunit b, mitochondrial	1.22%	1.60%
	O43707	Alpha-actinin-4	1.30%	1.30%
	O75947	ATP synthase subunit d, mitochondrial	1.36%	1.66%
	P08574	Cytochrome c1, heme protein, mitochondrial	1.41%	1.38%
	P21796	Voltage-dependent anion-selective channel protein 1	1.46%	1.55%
	Q13642	Four and a half LIM domains protein 1	1.55%	2.00%
	Q86TD4	Sarcalumenin	1.56%	1.81%
	P31930	Cytochrome b-c1 complex subunit 1, mitochondrial	1.74%	1.95%
	Q93084	Sarcoplasmic/endoplasmic reticulum calcium ATPase 3	1.77%	2.17%
	P20674	Cytochrome c oxidase subunit 5A, mitochondrial	1.80%	2.43%
	P14854	Cytochrome c oxidase subunit 6B1	1.80%	2.36%
	Q13423	NAD(P) transhydrogenase, mitochondrial	1.83%	1.99%
	P13073	Cytochrome c oxidase subunit 4 isoform 1, mitochondrial	1.84%	1.99%
	P06576	ATP synthase subunit beta, mitochondrial	1.84%	2.11%
	O14983	Sarcoplasmic/endoplasmic reticulum calcium ATPase 1	1.87%	2.27%
	P10606	Cytochrome c oxidase subunit 5B, mitochondrial	1.90%	2.26%
	P17612	cAMP-dependent protein kinase catalytic subunit alpha	1.94%	1.57%

(*Continued*)

Table 3. Continued

Gene ontology term: Biological Process Level 5	Accession number	Protein name	SKEW mean FSR (%/day)	BAL mean FSR (%/day)
	P16615	Sarcoplasmic/endoplasmicreticulum calcium ATPase 2	1.99%	2.37%
	O60936	Nucleolar protein 3	2.06%	3.97%
	P25705	ATP synthase subunit alpha, mitochondrial	2.14%	2.47%
	P54289	Voltage-dependent calcium channel subunit alpha-2/delta-1	2.26%	2.78%
	P08133	Annexin A6	2.68%	3.88%
	P54652	Heat shock-related 70 kDa protein 2	2.81%	2.88%
	P62258	14-3-3 protein epsilon	2.81%	3.74%
	P47985	Cytochrome b-c1 complex subunit Rieske, mitochondrial	3.04%	3.04%
	P21817	Ryanodine receptor 1	3.80%	5.18%
	P21333	Filamin-A	4.22%	4.17%
	Q93034	Cullin-5	4.23%	4.23%
	P02794	Ferritin heavy chain	4.74%	5.61%
	P13637	Sodium/potassium-transporting ATPase subunit alpha-3	6.26%	7.28%
	P50993	Sodium/potassium-transporting ATPase subunit alpha-2	6.43%	5.93%
	P13693	Translationally-controlled tumor protein	7.24%	11.95%
	P62158	Calmodulin	7.94%	8.64%
Nucleotide metabolic process GO:0009117, 81 proteins				
	O75964	ATP synthase subunit g, mitochondrial	0.59%	1.50%
	Q9P0J0	NADH dehydrogenase [ubiquinone] 1 alpha subcomplex subunit 13	0.62%	1.68%
	P00568	Adenylate kinase isoenzyme 1	0.83%	1.37%
	O95169	NADH dehydrogenase [ubiquinone] 1 beta subcomplex subunit 8, mitochondrial	0.84%	1.81%
	P00558	Phosphoglycerate kinase 1	1.05%	1.16%
	P54819	Adenylate kinase 2, mitochondrial	1.09%	1.63%
	Q99497	Protein DJ-1	1.11%	1.30%
	P30049	ATP synthase subunit delta, mitochondrial	1.14%	1.03%
	P48047	ATP synthase subunit O, mitochondrial	1.14%	1.32%
	P15259	Phosphoglycerate mutase 2	1.16%	1.23%
	P60174	Triosephosphate isomerase	1.17%	1.19%
	Q9NTK5	Obg-like ATPase 1	1.17%	1.72%
	Q08043	Alpha-actinin-3	1.20%	1.41%
	P99999	Cytochrome c	1.21%	2.43%
	P24539	ATP synthase subunit b, mitochondrial	1.22%	1.60%
	P06733	Alpha-enolase	1.23%	1.32%
	P13929	Beta-enolase	1.23%	1.26%
	Q9Y6M9	NADH dehydrogenase [ubiquinone] 1 beta subcomplex subunit 9	1.26%	1.14%
	O96000	NADH dehydrogenase [ubiquinone] 1 beta subcomplex subunit 10	1.31%	1.13%
	P09104	Gamma-enolase	1.32%	1.37%
	P06744	Glucose-6-phosphate isomerase	1.33%	1.63%
	P04406	Glyceraldehyde-3-phosphate dehydrogenase	1.33%	1.55%
	O75947	ATP synthase subunit d, mitochondrial	1.36%	1.66%
	P36871	Phosphoglucomutase-1	1.38%	1.45%
	P08574	Cytochrome c1, heme protein, mitochondrial	1.41%	1.38%
	Q9Y623	Myosin-4	1.43%	1.50%

(*Continued*)

Table 3. Continued

Gene ontology term: Biological Process Level 5	Accession number	Protein name	SKEW mean FSR (%/day)	BAL mean FSR (%/day)
	P13535	Myosin-8	1.47%	1.53%
	P11055	Myosin-3	1.52%	1.95%
	Q08623	Pseudouridine-5′-monophosphatase	1.54%	1.65%
	P23109	AMP deaminase 1	1.58%	1.45%
	P40925	Malate dehydrogenase, cytoplasmic	1.58%	1.41%
	P00338	L-Lactate dehydrogenase A chain	1.59%	1.92%
	P30085	UMP-CMP kinase	1.59%	2.53%
	P40926	Malate dehydrogenase, mitochondrial	1.60%	1.76%
	P03905	NADH-ubiquinone oxidoreductase chain 4	1.60%	1.78%
	O43674	NADH dehydrogenase [ubiquinone] 1 beta subcomplex subunit 5, mitochondrial	1.60%	1.47%
	P13533	Myosin-6	1.65%	1.64%
	P12883	Myosin-7	1.69%	1.67%
	P21695	Glycerol-3-phosphate dehydrogenase [NAD(+)], cytoplasmic	1.70%	1.93%
	P31930	Cytochrome b-c1 complex subunit 1, mitochondrial	1.74%	1.95%
	P04075	Fructose-bisphosphate aldolase A	1.77%	1.83%
	Q8TCD5	5′(3′)-Deoxyribonucleotidase, cytosolic type	1.78%	1.74%
	P22695	Cytochrome b-c1 complex subunit 2, mitochondrial	1.80%	1.81%
	P20674	Cytochrome c oxidase subunit 5A, mitochondrial	1.80%	2.43%
	P14854	Cytochrome c oxidase subunit 6B1	1.80%	2.36%
	P08559	Pyruvate dehydrogenase E1 component subunit alpha, somatic form, mitochondrial	1.81%	2.06%
	P09972	Fructose-bisphosphate aldolase C	1.82%	1.83%
	Q13423	NAD(P) transhydrogenase, mitochondrial	1.83%	1.99%
	P13073	Cytochrome c oxidase subunit 4 isoform 1, mitochondrial	1.84%	1.99%
	P06576	ATP synthase subunit beta, mitochondrial	1.84%	2.11%
	P24752	Acetyl-CoA acetyltransferase, mitochondrial	1.85%	1.86%
	P10606	Cytochrome c oxidase subunit 5B, mitochondrial	1.90%	2.26%
	P00403	Cytochrome c oxidase subunit 2	1.91%	2.14%
	P14618	Pyruvate kinase isozymes M1/M2	2.00%	2.23%
	P17858	6-Phosphofructokinase, liver type	2.09%	2.23%
	P25705	ATP synthase subunit alpha, mitochondrial	2.14%	2.47%
	P15531	Nucleoside diphosphate kinase A	2.21%	1.60%
	P22392	Nucleoside diphosphate kinase B	2.22%	2.19%
	P09622	Dihydrolipoyl dehydrogenase, mitochondrial	2.37%	2.56%
	O75489	NADH dehydrogenase [ubiquinone] iron-sulfur protein 3, mitochondrial	2.50%	2.96%
	Q9UI09	NADH dehydrogenase [ubiquinone] 1 alpha subcomplex subunit 12	2.63%	2.98%
	P30044	Peroxiredoxin-5, mitochondrial	2.67%	2.76%
	Q16718	NADH dehydrogenase [ubiquinone] 1 alpha subcomplex subunit 5	2.70%	3.06%
	O95168	NADH dehydrogenase [ubiquinone] 1 beta subcomplex subunit 4	2.77%	2.10%
	P19367	Hexokinase-1	2.83%	3.25%
	P11142	Heat shock cognate 71 kDa protein	2.88%	3.11%
	P47985	Cytochrome b-c1 complex subunit Rieske, mitochondrial	3.04%	3.04%

(*Continued*)

Table 3. Continued

Gene ontology term: Biological Process Level 5	Accession number	Protein name	SKEW mean FSR (%/day)	BAL mean FSR (%/day)
	P31040	Succinate dehydrogenase [ubiquinone] flavoprotein subunit, mitochondrial	3.07%	3.01%
	P49821	NADH dehydrogenase [ubiquinone] flavoprotein 1, mitochondrial	3.24%	3.01%
	P08237	6-Phosphofructokinase, muscle type	3.32%	3.63%
	O95182	NADH dehydrogenase [ubiquinone] 1 alpha subcomplex subunit 7	3.42%	3.46%
	O00217	NADH dehydrogenase [ubiquinone] iron-sulfur protein 8, mitochondrial	3.72%	3.18%
	O75306	NADH dehydrogenase [ubiquinone] iron-sulfur protein 2, mitochondrial	3.82%	3.82%
	P19404	NADH dehydrogenase [ubiquinone] flavoprotein 2, mitochondrial	3.92%	3.36%
	Q9UII2	ATPase inhibitor, mitochondrial	4.09%	5.25%
	Q02218	2-Oxoglutarate dehydrogenase, mitochondrial	4.28%	4.83%
	P28331	NADH-ubiquinone oxidoreductase 75 kDa subunit, mitochondrial	5.40%	5.56%
	O75251	NADH dehydrogenase [ubiquinone] iron-sulfur protein 7, mitochondrial	5.76%	8.23%
	P50993	Sodium/potassium-transporting ATPase subunit alpha-2	6.43%	5.93%
	P55072	Transitional endoplasmic reticulum ATPase	6.65%	8.49%
	P62158	Calmodulin	7.94%	8.64%

$^{13}C_6$ Phe infusion trials (Murphy *et al.* 2015) participants rested in the supine position. It is well established that inactivity suppresses MyoPS and this probably contributed to the lower rates of MyoPS measured acutely compared to the free-living D_2O measurements wherein participants performed their usual daily activity (Breen *et al.* 2013). Moreover, in the acute study (Murphy *et al.* 2015) MyoPS in the ER + RT condition was measured 48 h after the last resistance exercise session. As MyoPS content is greatest immediately after exercise and wanes over time it is unsurprising that acute rates were lower than the free-living D_2O rates which captured the integrated response to six RT sessions performed over the 2 weeks of ER + RT.

Our most novel finding is that performance of RT during ER increases the synthesis of most (175 of 190 measured) individual skeletal muscle proteins in the myofibrillar, sarcoplasmic and mitochondrial protein categories, compared to ER alone. To the best of our knowledge, we are the first to report the synthetic rates of a large number of individual skeletal muscle proteins in humans in response to RT during ER. Our data indicate that, even in the presence of ER, performance of RT elevated the synthesis rates of a broad array of individual skeletal muscle proteins across the proteome, including not only contractile proteins but also sarcoplasmic and mitochondrial proteins (Table 1; Fig. 3) and proteins across many gene ontologies (Fig. 5). This 'mass response' appears inconsistent with the phenotype induced by prolonged RT (i.e. myofibrillar protein accretion). Nevertheless, previous work suggests that the specificity of the muscle protein synthetic response following an acute bout of resistance exercise is dependent on training status (Kim *et al.* 2005; Wilkinson *et al.* 2008). For example, an acute bout of resistance exercise stimulated mitochondrial, as well as myofibrillar, protein synthesis in untrained men, whereas the increase in mitochondrial protein synthesis was absent after 10 weeks of RT (Wilkinson *et al.* 2008). As our individual FSR measurements reflect the integrated response to six resistance exercise sessions in previously untrained participants it may be that this 'mass response' reflects an early, less specific muscle protein synthetic response to RT. As such, it remains possible that the response may become more specific to myofibrillar proteins after a prolonged period of training. Camera *et al.* (2017) recently used deuterated water to measure the turnover of individual skeletal muscle proteins in response to RT over an integrated 9 day period in overweight young men consuming a high-fat low-carbohydrate diet. While the authors reported a less 'global' response across the proteome (i.e. 28 of the 90 measured proteins were

RT-responsive compared to 175 of 190 proteins in the present study) increases in the synthesis of both sarcoplasmic and myofibrilliar proteins were observed (Camera *et al.* 2017). This is consistent with the notion that, at least early in RT, muscle protein synthetic responses are not confined to contractile and structural components.

The ability to discern the FSR for individual skeletal muscle proteins, rather than global tissue or even sub-fractional synthetic rates, provides unique insight into the response to an intervention that would otherwise not be possible. Indeed, our data and others (Camera *et al.* 2017) demonstrate dramatic variability in protein turnover rates, highlighting that sub-fractional analysis may mask dynamic changes in individual proteins within a tissue fraction. The potential applications of proteome dynamic techniques are far reaching and future work could, potentially, lead to the identification of a 'biological blueprint' of the skeletal muscle response to RT or other interventions (Hawley & Krook, 2016). This could have important implications for optimizing exercise and other treatment interventions for the prevention and management of sarcopenia as well as other musculoskeletal conditions.

Consistent with our findings of increased synthesis rates of the majority of individual skeletal muscle proteins measured in response to ER + RT compared to ER alone, we report a clear effect of RT on integrative bulk MyoPS during ER in older men. Illustrating the potency of this stimulus, we observed that just six sessions of low-load RT performed over 2 weeks was sufficient to increase longer-term bulk MyoPS by ∼26% compared to ER alone. This finding is in line with our acute data showing higher

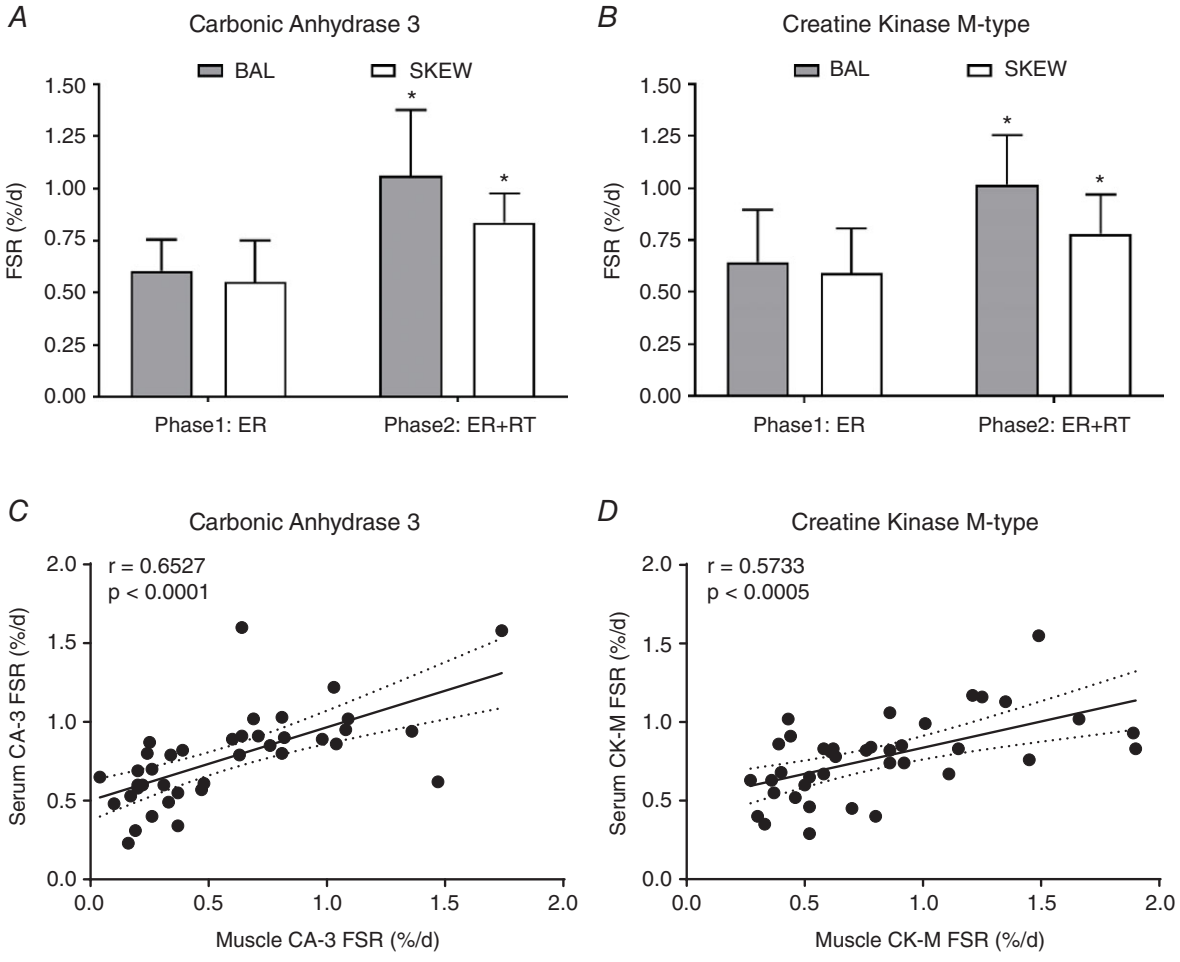

Figure 6. Carbonic anhydrase 3 (*A*) and creatine kinase M-type (*B*) fractional synthesis in serum of SKEW and BAL participants ($n = 10$ per group) during 2 weeks of energy restriction (Phase1: ER) and 2 weeks of energy restriction + resistance training (Phase2: ER + RT)

*Different from Phase 1: ER; $P < 0.05$; two-way ANOVA with *post-hoc* Holm–Sidak comparison. Values are mean ± SD. Relationship between carbonic anhydrase 3 (*C*) and creatine kinase M-type (*D*) fractional synthetic rates (FSR; %/day) measured in the serum and in the muscle using D_2O labelling in overweight and obese older men who underwent 2 weeks of energy restriction (Phase 1) and 2 weeks of energy restriction + resistance training (Phase 2) with balanced (BAL) or skewed (SKEW) protein distribution.

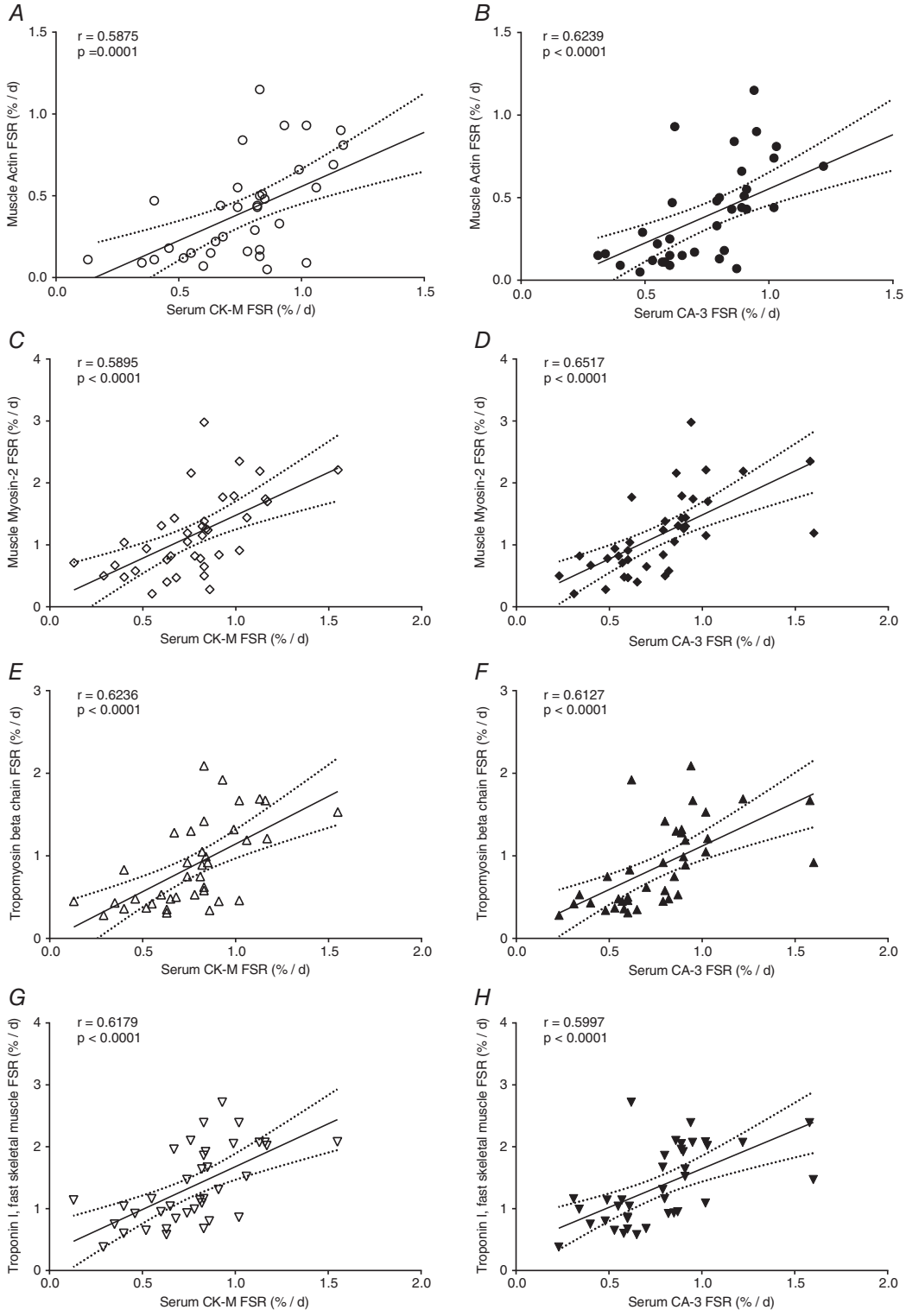

Figure 7. Relationship between carbonic anhydrase 3 and creatine kinase M-type fractional synthetic rates (FSR; %/day) measured in the serum and the myofibrillar proteins (actin, myosin, tropomyosin, troponin) fractional synthetic rates (FSR; %/day), measured in the muscle using D_2O labelling in overweight and obese older men who underwent 2 weeks of energy restriction (Phase 1) and 2 weeks of energy restriction + resistance training (Phase 2) with balanced (BAL) or skewed (SKEW) protein distribution

Table 4. Comparison between myofibrillar protein fractional synthetic rate (FSR, %/day) measured via L-[ring-$^{13}C_6$]-phenylalanine infusion and D_2O

	ER		ER + RT	
	$^{13}C_6$ Phe	D_2O	$^{13}C_6$ Phe	D_2O
BAL (%/day)	0.89 ± 0.11*	1.24 ± 0.31†	1.01 ± 0.06*	1.64 ± 0.48†
SKEW (%/day)	0.82 ± 0.11*	1.26 ± 0.37†	0.90 ± 0.11*	1.52 ± 0.66†

Values are means ± SD ($n = 10$ per group). BAL, balanced protein intake group; ER, energy restriction; ER + RT, energy restriction plus resistance training; FSR, fractional synthetic rate; Phe, phenylalanine; SKEW, skewed protein intake group.
*Based on previously reported rates measured acutely over an 11 h labelling period in response to BAL or SKEW pattern of protein intake at the end of 2 weeks of ER and 2 weeks of ER + RT (Murphy *et al*. 2015). Acute FSRs were converted from %/h to %/day by assuming that approximately 16 h per day are spent in the postprandial state and 8 h in the postabsorptive state in Western countries.
†Data represent integrated FSR measured over the 2 weeks of ER and 2 weeks of ER + RT in the BAL and SKEW protein intake groups. The same participants were included in the L-[ring-$^{13}C_6$]-phenylalanine infusion and D_2O measurements.

rates of bulk MyoPS at the end of ER + RT *versus* ER (Murphy *et al.* 2015) and supports previous work showing that the incorporation of RT can attenuate muscle mass loss during ER in older adults (Campbell *et al.* 2009; Villareal *et al.* 2017).

Further illustrating the potential application of proteome kinetics and the 'virtual biopsy' approach (using kinetic measurements on proteins released into body fluids to reveal kinetics of synthesis or turnover of these proteins back in the tissue of origin), we observed a correlation between the synthetic rates of skeletal muscle-derived (synthesized) proteins obtained via serum sampling (CK-M, CA-3) and the synthetic rates of proteins obtained via skeletal muscle sampling (CK-M, CA-3, actin, myosin, tropomyosin, troponin). This suggests that measuring synthetic rates of blood-borne skeletal muscle proteins could act as a surrogate for the direct (but invasive) measurement of skeletal muscle protein synthesis. While changes in MPS occur rapidly (hours) in response to anabolic interventions, changes in muscle mass, strength and function occur far more slowly (months to years). The measurement of MPS requires muscle biopsies, making it generally impractical for routine use in therapeutic trials or clinical practice. Our data corroborate recent reports that the FSR of CK-M and CA-3 isolated from serum correlated with the FSR of CK-M and CA-3, and numerous other proteins of various ontologies, in skeletal muscle in clinical and preclinical studies (Shankaran *et al.* 2016*a*, *b*). Taken together, these data suggest that measuring the FSR of blood-borne skeletal muscle proteins (such as serum CK-M and CA-3) may have the potential to act as a minimally invasive biomarker of MPS. It should be noted that FSR of serum CA-3 and CK-M were higher during ER + RT compared to ER ($P < 0.001$ main effect for phase), and thus were sensitive enough to reveal effects on RT on skeletal muscle FSR. Given the wide variability in individual responses to anabolic interventions such as standardized exercise training programmes and pharmaceutical interventions, such an approach could allow for the early identification of responders and non-responders so that training/treatment can be personalized to confer maximum musculoskeletal benefits. Nevertheless, further work will be needed to validate this approach and to investigate if it is sensitive enough to identify small, but clinically relevant, changes in MPS.

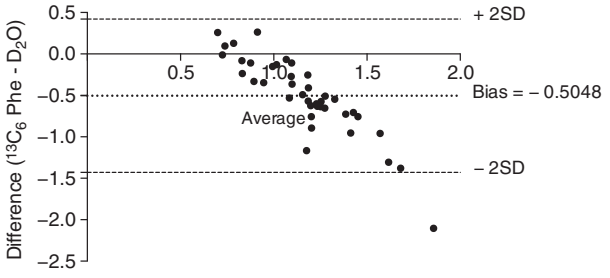

Figure 8. Bland–Altman plot of comparison between myofibrillar protein fractional synthetic rate (FSR) measured acutely via l-[ring-$^{13}C_6$]-phenylalanine infusion (Murphy *et al*. 2015) and over 2 weeks via D_2O
Acute FSR was converted from %/h to %/day assuming that approximately 16 h per day are spent in the postprandial state and 8 h in the postabsorptive state in Western countries.

A potential limitation of our study is that we did not measure longer-term MyoPS at baseline while the participants were in EB. It is therefore unclear whether there were ER-induced changes in longer-term integrated bulk MyoPS compared to the absence of ER. In our previous study we measured acute bulk MyoPS at baseline in EB and showed that RT combined with a balanced, but not a skewed, distribution of protein ingestion restored the lower fed-state rates of acute bulk MyoPS during ER to the higher EB levels (Murphy *et al.* 2015).

Another limitation is that we did not measure the change in abundance of individual skeletal muscle proteins. As such, we are unable to determine whether the increases in individual protein FSR translated to protein accretion or simply reflected enhanced turnover. A few

points are worth noting in this regard. First, the abundance of a protein is typically measured per gram of tissue (measured weight) or by comparison to abundances of other proteins (e.g. by label-free methods). Anabolic interventions may not change the relative abundances of the major proteins in skeletal muscle, however. In settings of global muscle mass increase, where all proteins may increase in proportion and the concentration of most proteins per gram of tissue does not change, abundance measurements are therefore in principle different from, and less sensitive, than fractional synthesis rates, which are independent of tissue mass or relative amount of other proteins present. Muscle may accrue as a unit without changes in composition, in which case the true metric of abundance change for a protein in this setting is total amount of muscle tissue, which is a macroscopic measurement and not a biochemical measurement. In addition, the relatively short duration of the intervention (2 weeks) may not have been long enough to result in changes in pool sizes or mass of muscle proteins. Changes in mass may lag behind changes in synthesis rates, so a relationship is not always immediately apparent.

Moreover, at the global tissue level, it is generally accepted that the response of MPS to RT and feeding is the principal driver of the 'anabolic' shift towards a positive net protein balance with a comparatively small contribution from the reduction in muscle protein breakdown. Nevertheless, using label-free methods, Camera *et al.* (2017) recently reported no increase in abundance despite an increase in turnover for several individual skeletal muscle proteins in response to short-term RT in young men. An important point, however, is that even if the increase in individual protein synthetic rates we observed in the present study were due to increased turnover without enhanced abundance, this may still reflect a positive outcome by supporting protein renewal and preventing the accumulation of old/damaged components (Lopez-Otin *et al.* 2013).

Some potential technical limitations are worth noting. We subtracted out isotopic label present in each peptide at the end of the first 2-week labelling period (Phase 1), so that the end of the initial labelling period served as a new baseline for rise-to-plateau label incorporation. This correction is necessary for a continuous labelling approach with two time-points, but subtraction of a second baseline may have added to experimental variability. In addition, we used time-averaged D_2O exposure for the precursor pool rather than using a kinetic model (Price *et al.* 2012) in which linked pools of body water and peptides each acquire time-varying deuterium label with fitted turnover rates. To compare kinetic results using time-averaged D_2O exposure to the previous kinetic modelling approach, we analysed isotopic data from two proteins (CA-3 and CK-M in serum) by the two methods. A good correlation (slope of 1.02) was observed between the FSRs derived by kinetic modelling and the simplified calculation, for the 20 study participants. This indicates that under these conditions of short labelling times and stable body D_2O enrichments, in the setting of relatively slow protein synthesis rates, the approximation of time-averaged D_2O exposure does not result in a calculated FSR that is systematically different from a kinetic model in which the body water enrichment calculation is more complex.

In conclusion, we report little influence of the pattern of protein ingestion over the day on the integrated rate of bulk MyoPS measured over 2 weeks of ER alone or 2 weeks of ER + RT in overweight/obese older men, although subtle differences in the pattern of individual protein synthesis rates in skeletal muscle were apparent between the dietary interventions. We provide novel data showing that short-term RT increases both the synthesis rates of the majority of individual skeletal muscle proteins measured, comprising many gene ontologies, and longer-term integrated bulk MyoPS under conditions of ER in older adults.

References

Baumgartner RN, Wayne SJ, Waters DL, Janssen I, Gallagher D & Morley JE (2004). Sarcopenic obesity predicts instrumental activities of daily living disability in the elderly. *Obes Res* **12**, 1995–2004.

Bouchonville MF & Villareal DT (2013). Sarcopenic obesity: how do we treat it? *Curr Opin Endocrinol Diabetes Obes* **20**, 412–419.

Breen L, Stokes KA, Churchward-Venne TA, Moore DR, Baker SK, Smith K, Atherton PJ & Phillips SM (2013). Two weeks of reduced activity decreases leg lean mass and induces "anabolic resistance" of myofibrillar protein synthesis in healthy elderly. *J Clin Endocrinol Metab* **98**, 2604–2612.

Burke LM, Winter JA, Cameron-Smith D, Enslen M, Farnfield M & Decombaz J (2012). Effect of intake of different dietary protein sources on plasma amino acid profiles at rest and after exercise. *Int J Sport Nutr Exerc Metab* **22**, 452–462.

Busch R, Kim YK, Neese RA, Schade-Serin V, Collins M, Awada M, Gardner JL, Beysen C, Marino ME, Misell LM & Hellerstein MK (2006). Measurement of protein turnover rates by heavy water labeling of nonessential amino acids. *Biochim Biophys Acta* **1760**, 730–744.

Camera DM, Burniston JG, Pogson MA, Smiles WJ & Hawley JA (2017). Dynamic proteome profiling of individual proteins in human skeletal muscle after a high-fat diet and resistance exercise. *FASEB J* **31**, 5478–5494.

Campbell WW, Haub MD, Wolfe RR, Ferrando AA, Sullivan DH, Apolzan JW & Iglay HB (2009). Resistance training preserves fat-free mass without impacting changes in protein metabolism after weight loss in older women. *Obesity (Silver Spring)* **17**, 1332–1339.

Chung JY, Kang HT, Lee DC, Lee HR & Lee YJ (2013). Body composition and its association with cardiometabolic risk factors in the elderly: a focus on sarcopenic obesity. *Arch Gerontol Geriatr* **56**, 270–278.

Conley TB, Apolzan JW, Leidy HJ, Greaves KA, Lim E & Campbell WW (2011). Effect of food form on postprandial plasma amino acid concentrations in older adults. *Br J Nutr* **106**, 203–207.

Cuthbertson D, Smith K, Babraj J, Leese G, Waddell T, Atherton P, Wackerhage H, Taylor PM & Rennie MJ (2005). Anabolic signaling deficits underlie amino acid resistance of wasting, aging muscle. *FASEB J* **19**, 422–424.

Diouf I, Charles MA, Ducimetiere P, Basdevant A, Eschwege E & Heude B (2010). Evolution of obesity prevalence in France: an age-period-cohort analysis. *Epidemiology* **21**, 360–365.

Flegal KM, Carroll MD, Kit BK & Ogden CL (2012). Prevalence of obesity and trends in the distribution of body mass index among US adults, 1999–2010. *JAMA* **307**, 491–497.

Gutierrez-Fisac JL, Guallar-Castillon P, Leon-Munoz LM, Graciani A, Banegas JR & Rodriguez-Artalejo F (2012). Prevalence of general and abdominal obesity in the adult population of Spain, 2008–2010: the ENRICA study. *Obes Rev* **13**, 388–392.

Hawley JA & Krook A (2016). Metabolism: one step forward for exercise. *Nat Rev Endocrinol* **12**, 7–8.

Hector AJ, Marcotte GR, Churchward-Venne TA, Murphy CH, Breen L, von Allmen M, Baker SK & Phillips SM (2015). Whey protein supplementation preserves postprandial myofibrillar protein synthesis during short-term energy restriction in overweight and obese adults. *J Nutr* **145**, 246–252.

Janssen I, Baumgartner RN, Ross R, Rosenberg IH & Roubenoff R (2004). Skeletal muscle cutpoints associated with elevated physical disability risk in older men and women. *Am J Epidemiol* **159**, 413–421.

Kim J, Wang Z, Heymsfield SB, Baumgartner RN & Gallagher D (2002). Total-body skeletal muscle mass: estimation by a new dual-energy X-ray absorptiometry method. *Am J Clin Nutr* **76**, 378–383.

Kim PL, Staron RS & Phillips SM (2005). Fasted-state skeletal muscle protein synthesis after resistance exercise is altered with training. *J Physiol* **568**, 283–290.

Landi F, Liperoti R, Russo A, Giovannini S, Tosato M, Barillaro C, Capoluongo E, Bernabei R & Onder G (2013). Association of anorexia with sarcopenia in a community-dwelling elderly population: results from the ilSIRENTE study. *Eur J Nutr* **52**, 1261–1268.

Lopez-Otin C, Blasco MA, Partridge L, Serrano M & Kroemer G (2013). The hallmarks of aging. *Cell* **153**, 1194–1217.

Mathus-Vliegen EM (2012). Prevalence, pathophysiology, health consequences and treatment options of obesity in the elderly: a guideline. *Obesity Facts* **5**, 460–483.

Moore DR, Churchward-Venne TA, Witard O, Breen L, Burd NA, Tipton KD & Phillips SM (2015). Protein ingestion to stimulate myofibrillar protein synthesis requires greater relative protein intakes in healthy older versus younger men. *J Gerontol A Biol Sci Med Sci* **70**, 57–62.

Moore DR, Tang JE, Burd NA, Rerecich T, Tarnopolsky MA & Phillips SM (2009). Differential stimulation of myofibrillar and sarcoplasmic protein synthesis with protein ingestion at rest and after resistance exercise. *J Physiol* **587**, 897–904.

Murphy CH, Churchward-Venne TA, Mitchell CJ, Kolar NM, Kassis A, Karagounis LG, Burke LM, Hawley JA & Phillips SM (2015). Hypoenergetic diet-induced reductions in myofibrillar protein synthesis are restored with resistance training and balanced daily protein ingestion in older men. *Am J Physiol Endocrinol Metab* **308**, E734–743.

Neese RA, Siler SQ, Cesar D, Antelo F, Lee D, Misell L, Patel K, Tehrani S, Shah P & Hellerstein MK (2001). Advances in the stable isotope-mass spectrometric measurement of DNA synthesis and cell proliferation. *Anal Biochem* **298**, 189–195.

Nicklas BJ, Cesari M, Penninx BW, Kritchevsky SB, Ding J, Newman A, Kitzman DW, Kanaya AM, Pahor M & Harris TB (2006). Abdominal obesity is an independent risk factor for chronic heart failure in older people. *J Am Geriatr Soc* **54**, 413–420.

Parr EB, Coffey VG & Hawley JA (2013). 'Sarcobesity': a metabolic conundrum. *Maturitas* **74**, 109–113.

Price JC, Holmes WE, Li KW, Floreani NA, Neese RA, Turner SM & Hellerstein MK (2012). Measurement of human plasma proteome dynamics with ^2H_2O and liquid chromatography tandem mass spectrometry. *Anal Biochem* **420**, 73–83.

Rennie MJ, Smith K & Watt PW (1994). Measurement of human tissue protein synthesis: an optimal approach. *Am J Physiol Endocrinol Metab* **266**, E298–307.

Robinson MM, Turner SM, Hellerstein MK, Hamilton KL & Miller BF (2011). Long-term synthesis rates of skeletal muscle DNA and protein are higher during aerobic training in older humans than in sedentary young subjects but are not altered by protein supplementation. *FASEB J* **25**, 3240–3249.

Rossi A, Fantin F, Di Francesco V, Guariento S, Giuliano K, Fontana G, Micciolo R, Solerte SB, Bosello O & Zamboni M (2008). Body composition and pulmonary function in the elderly: a 7-year longitudinal study. *Int J Obes (Lond)* **32**, 1423–1430.

Scalzo RL, Peltonen GL, Binns SE, Shankaran M, Giordano GR, Hartley DA, Klochak AL, Lonac MC, Paris HL, Szallar SE, Wood LM, Peelor FF, 3rd, Holmes WE, Hellerstein MK, Bell C, Hamilton KL & Miller BF (2014). Greater muscle protein synthesis and mitochondrial biogenesis in males compared with females during sprint interval training. *FASEB J* **28**, 2705–2714.

Shankaran M, King CL, Angel TE, Holmes WE, Li KW, Colangelo M, Price JC, Turner SM, Bell C, Hamilton KL, Miller BF & Hellerstein MK (2016*a*). Circulating protein synthesis rates reveal skeletal muscle proteome dynamics. *J Clin Invest* **126**, 288–302.

Shankaran M, Shearer TW, Stimpson SA, Turner SM, King C, Wong PA, Shen Y, Turnbull PS, Kramer F, Clifton L, Russell AJ, Hellerstein MK & Evans WJ (2016*b*). Proteome-wide muscle protein fractional synthesis rates predict muscle mass gain in response to a selective androgen receptor modulator in rats. *Am J Physiol Endocrinol Metab* **310**, E405–417.

Turner SM, Murphy EJ, Neese RA, Antelo F, Thomas T, Agarwal A, Go C & Hellerstein MK (2003). Measurement of TG synthesis and turnover in vivo by ^2H_2O incorporation into the glycerol moiety and application of MIDA. *Am J Physiol Endocrinol Metab* **285**, E790–803.

Vasquez E, Batsis JA, Germain CM & Shaw BA (2014). Impact of obesity and physical activity on functional outcomes in the elderly: data from NHANES 2005–2010. *J Aging Health* **26**, 1032–1046.

Villareal DT, Aguirre L, Gurney AB, Waters DL, Sinacore DR, Colombo E, Armamento-Villareal R & Qualls C (2017). Aerobic or resistance exercise, or both, in dieting obese older adults. *N Engl J Med* **376**, 1943–1955.

Waters DL, Ward AL & Villareal DT (2013). Weight loss in obese adults 65years and older: a review of the controversy. *Exp Gerontol* **48**, 1054–1061.

West DW, Burd NA, Coffey VG, Baker SK, Burke LM, Hawley JA, Moore DR, Stellingwerff T & Phillips SM (2011). Rapid aminoacidemia enhances myofibrillar protein synthesis and anabolic intramuscular signaling responses after resistance exercise. *Am J Clin Nutr* **94**, 795–803.

Wilkinson DJ, Cegielski J, Phillips BE, Boereboom C, Lund JN, Atherton PJ & Smith K (2015). Internal comparison between deuterium oxide (D_2O) and L-[ring-13C6] phenylalanine for acute measurement of muscle protein synthesis in humans. *Physiol Rep* **3**, e12433.

Wilkinson DJ, Franchi MV, Brook MS, Narici MV, Williams JP, Mitchell WK, Szewczyk NJ, Greenhaff PL, Atherton PJ & Smith K (2014). A validation of the application of D_2O stable isotope tracer techniques for monitoring day-to-day changes in muscle protein subfraction synthesis in humans. *Am J Physiol Endocrinol Metab* **306**, 571–579.

Wilkinson SB, Phillips SM, Atherton PJ, Patel R, Yarasheski KE, Tarnopolsky MA & Rennie MJ (2008). Differential effects of resistance and endurance exercise in the fed state on signalling molecule phosphorylation and protein synthesis in human muscle. *J Physiol* **586**, 3701–3717.

Additional information

Competing interests

Both AK and LGK are employees of Nestec SA, a subsidiary of Nestle, which was a linkage partner in the grant for this study.

Author contributions

CHM, AK, LGK, LMB, JAH and SMP conceived and designed the research; CHM, TAC-V, CJM, NMK, MS, CK, KL, MH and SMP generated and collected data; CHM, SMP, MS, KL and MH analysed data, CHM, MS, MH and SMP interpreted the results; CHM and MS prepared the figures; CHM, MS, MH and SMP wrote the manuscript; CHM, TAC-V, CJM, AK, LGK, LMB, JAH, MS, K, MH and SMP revised the manuscript and approved the final version.

Funding

This study was funded by an Australian Research Council Linkage Project grant (LP100100010) to JAH, Nestle and the Australian Institute of Sport, a National Science and Engineering Research Council of Canada grant to SMP and KineMed, Inc.

Acknowledgements

We thank Tracy Rerecich and Todd Prior for their technical and laboratory assistance and the study participants for their time and dedication. We also would like to acknowledge the contribution from Thomas Angel PhD and Marc Colangelo PhD to the data analyses; Scott Turner PhD for initial discussions as well as Joan Protasio and Chancy Fessler for technical assistance.